Natural Hazards
https://doi.org/10.1007/s11069-025-07262-8

ORIGINAL PAPER

Factors influencing landslide occurrence in low-relief formerly glaciated landscapes: landslide inventory and susceptibility analysis in Minnesota, USA

Laura D. Triplett[1] · Morena N. Hammer[2] · Stephen B. DeLong[2] · Karen B. Gran[3] · Carrie E. Jennings[4] · Zachary T. Engle[5] · Julie K. Bartley[1] · Dylan J. Blumentritt[6] · Andy J. Breckenridge[7] · Stephanie Day[8] · Melissa A. Kohout[9] · Phil H. Larson[9] · Jeni A. McDermott[10] · Emilie M. Richard[3]

Received: 19 December 2024 / Accepted: 22 March 2025

Abstract
In landscapes recently impacted by continental glaciation, landslides may occur where topographic relief has been generated by the drainage of glacial lakes and ensuing post-glacial fluvial network development into unconsolidated glacially derived sediments and exhumed bedrock. To investigate linkages among environmental variables, post-glacial landscape development, and landslides, we created a landslide inventory of nearly 10,000 landslides in five regions of the formerly glaciated low-relief state of Minnesota, United States. Multivariate logistic regression indicates the importance of slope angle, lithology, and the development of stream valleys to landslide distribution. Areas underlain by fine-grained glaciolacustrine and nearshore deposits that are incised by streams are particularly prone to shallow (< 1–2 m depth) landslides. Landslides also occur in a wide range of glacial and fluvial deposits, and as rockfall in layered Paleozoic sedimentary rocks in central and southern Minnesota and Precambrian igneous and sedimentary rocks in north-eastern Minnesota. Although no more than 1–2% of the studied regions are susceptible to landslides, they can pose risk to life and safety, damage infrastructure, and impact water quality. The combination of recently generated low-relief steep slopes, extensive unconsolidated sediments, and layered sedimentary bedrock make this formerly glaciated landscape more susceptible to landslides than current national-scale models indicate.

Keywords Landslide inventory · Susceptibility model · Post-glacial landscape · Minnesota · Quaternary sediments · Low relief

Extended author information available on the last page of the article

1 Introduction

During the Pleistocene, high latitude areas around the world were impacted by repeated continental glaciation. Much of this area is low relief, but somewhat counter-intuitively, now hosts extensive landslide activity and landforms. Glacial till, sand and gravel, fine-grained glaciolacustrine sediments, and aeolian deposits form the near-surface stratigraphy in these areas providing thick sequences of unconsolidated sediment in which landslides may occur. In addition, many post-glacial landscapes have been impacted by incision resulting from drainage of proglacial lakes, and to a lesser extent, differential isostatic rebound and drainage basin reorganization. The base level fall initiated by these events can lead to ongoing incision of tributary stream networks, characterized by the headward erosion of stream channels into adjacent areas, establishment of steep bluffs along stream valleys, and deepening and widening of these valleys as channel networks develop (Cossart et al. 2013; Gran et al. 2013; Breckenridge 2013; Faulkner et al. 2016; Wickert et al. 2019; Hilgendorf et al. 2020). These processes combine to form areas with steep slopes and predominantly weak substrates, particularly within river valleys and along lakeshores (Mickelson et al. 1977; Swenson et al. 2006; Kohv et al. 2009; Day et al. 2013; Gran et al. 2013; Cloutier et al. 2016; Wartman et al. 2016; Perkins et al. 2017; Krueger et al. 2020).

We report on the occurrence of landslides in the state of Minnesota, United States, an area greatly impacted by continental glaciation. We explain how the distribution and type of landslides relate to glacial and post-glacial processes and present an analysis of the susceptibility to future landslides. This work was motivated by recent landslides in Minnesota that caused fatalities (e.g. Associated Press 2023), heavy precipitation and flooding events that caused extensive landsliding (e.g. DeLong et al. 2022a, b), and, more generally, the need to understand hazards associated with ongoing landslide activity. This is the first holistic study of landslides in Minnesota and may serve as the basis for future site-specific hazard characterization and mitigation. The fundamental data that underlie these analyses are in a recently published landslide inventory of five regions of Minnesota (DeLong et al. 2021), although we expand on those data with interpretations made from field observations here. To generate the inventory, we used lidar-derived topographic data to map landslides according to their morphology, researched historical reports of landslide activity, and performed field investigations. We used the landslide inventory along with other available statewide data such as the near-surface lithologies, slope, distance-to-stream, and depth-to-bedrock to generate the landslide susceptibility analyses presented here.

Landslide hazard research efforts involving generation of landslide inventories and analysis of landslide susceptibility are common. Landslide inventories in the United States are synthesized in Belair et al. (2022), procedures for generating landslide inventories from lidar data are found in Burns and Madin (2009), and a review of the utility of landslide inventories can be found in Guzzetti et al. (2012). Many reviews of landslide susceptibility analysis describe statistical, machine learning, and other quantitative and qualitative methods (e.g. Reichenbach et al. 2018; Liu et al. 2023; Pathak et al. 2023). National-scale susceptibility modeling for the United States is described in Mirus et al. (2024).

Previous work assessing landslide hazards in Minnesota is lacking. Mohseni et al. (2018) report a proof-of-concept pilot study describing the use of statewide data for landslide susceptibility modeling in two counties. Several regional studies associated with the research described here are among the first to look at the widespread occurrence of landslides for

Minnesota (Jennings et al. 2016, 2020; Dean 2018; Kohout 2019; Richard 2020; DeLong et al. 2022a, b). DeLong et al. (2021) is the first regional-scale landslide inventory to be published for Minnesota. Shafer et al. (2024) present a similar study for the neighboring low-relief areas in North Dakota.

Landslide inventories and susceptibility maps can help guide zoning, land use and infrastructure development, assist with implementation of emergency management plans, and educate the public regarding landslide hazards (Kirschbaum et al. 2010; Kirschbaum and Stanley 2018; Mirus et al. 2020, 2024). Most research on landslides and landslide susceptibility focuses on tectonically active and mountainous environments across the globe (e.g. Korup et al. 2007; Reichenbach et al. 2018). However, landscapes with low and moderate relief can be prone to significant landslide hazards, especially where steep slopes are formed in unconsolidated sediments (Korup et al. 2007; Pánek 2015; Geertsema et al. 2017; Shafer et al. 2024). Susceptibility models at the national scale fail to capture all the details in many of these high susceptibility zones (Mirus et al. 2020, 2024), highlighting a need for studies like this that investigate the specific factors causing landslides in regions of low relief that contain slopes steepened due to geologically recent changes in topographic base-level.

2 Study area

The State of Minnesota is located within the Central Lowlands and Superior Upland physiographic provinces of the United States (U.S. Geological Survey 2023). The region was glaciated multiple times during the Quaternary, creating a low-relief landscape with limited exposure of bedrock (Lusardi et al. 2019). The most recent glaciation buried or modified landscapes and drainage networks formed during pre-glacial and interglacial times, although part of southeastern Minnesota remained ice free during the most recent Wisconsinan glaciation (Johnson et al. 2016). The repeated glacial advances and retreats left a mosaic of poorly consolidated sediments at the surface.

As ice melted, proglacial lakes formed, and then drained through spillways that carried large meltwater floods downstream. Late- and post-glacial lake drainage and fluvial incision created most of the topographic relief in the state and are the focus areas for landslides on the most recently formed river and lakeshore slopes as they continue to evolve (e.g. Anderson et al. 2023). Other relief was formed in ice stagnation landscapes, on glacial depositional landforms, and in areas such as the Lake Superior basin where glaciers eroded more deeply into the substrate. The largest of the proglacial lakes formed was glacial Lake Agassiz, which eventually overflowed and drained downslope carving a valley now occupied by the Minnesota River and setting the course of the modern valley (Fig. 1). The formations of the spillway lowered the base level to which post-glacial fluvial systems continue to respond with incision migrating upstream over time through head-cutting and knickpoint migration (Gran et al. 2013; Faulkner et al. 2016).

The study area consists of five landslide-prone regions in the northwestern, northeastern, south-central, and southeastern parts of Minnesota (Fig. 1). Together, the mapped areas comprise 41% of the state. The five regions were delineated based on apparent differences in the character of the landscape. In detail, the boundaries between some regions were chosen along county lines. This was done simply to facilitate division of labor and data among the

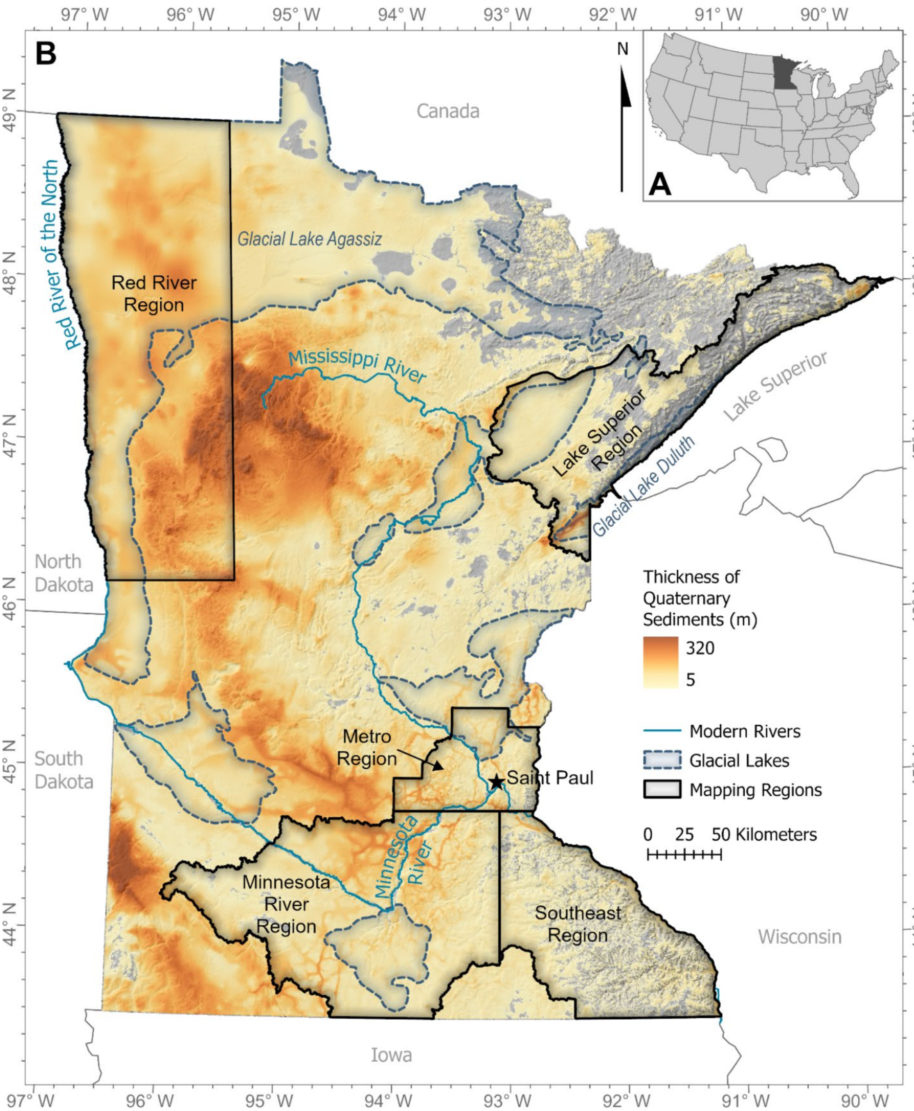

Fig. 1 Study Area. The base map shows thickness of Quaternary deposits (Jirsa et al. 2011), with the area mapped for each of the five regions delineated by shaded lines. Dashed blue lines indicate approximate boundaries of former pro-glacial lakes present at the time of deglaciation, some of which are labeled on the map. (adapted from Johnson et al. 2016). The modern Mississippi River and Minnesota River are indicated in blue (MN DNR 2013a). Underlying map is exaggerated hillshade (z = 30) (European Space Agency 2021), and where Quaternary deposits are < 5 m thick this hillshade map is depicted in light gray. Light gray lines mark adjacent state boundaries

research team in areas where the changes in landscape character was gradational (e.g. Minnesota River Region to Metro Region).

More detailed regional characterization follows here and in Table 1:

1. The **Southeast Region** has the greatest relief and thinnest sediment cover. Extensive areas remained ice-free during the Wisconsinan glaciation (~100–11 ka years before present). However, the entire region was glaciated during Illinoian or pre-Illinoian glaciations (Jennings and Johnson 2011; Lusardi et al. 2019). The uplands generally correspond with the elevation of flat-lying, erosion-resistant Cambrian and Ordovician limestone and dolostone (Mossler 2008) that overlie more erodible shales and sandstones (Runkel 1996). These bedrock units are exposed along the river bluffs. The low-relief uplands tend to be underlain by <3 m thick cover of glacial sediment (Lusardi et al. 2019), and the loess thickens towards the Mississippi River (Mason et al. 1994). The Mississippi River is the base level for tributaries, which have valley floors up to 1600 m wide in the lowest reaches of the largest sub-watersheds.
2. The **Metro Region** is underlain by Upper Ordovician sedimentary bedrock, with low overall relief and a highly variable glacial sediment cover (up to 180 m thick). It includes portions of the Mississippi River and Minnesota River valleys up- and downstream of their confluence in the Minneapolis-Saint Paul metropolitan area. Approximately 40 m of relief exposes the glacial sediments and, where present, the flat-lying Upper Ordovician shale, limestone, and sandstone (Mossler 2008). The relief was originated by the catastrophic overflow drainage from glacial Lake Agassiz through what is the modern Minnesota River valley. The knickpoints generated by that incision have migrated upstream on the Mississippi and Minnesota rivers and their tributaries, generating much of the relief in this region today.
3. The **Minnesota River Region** lies in south-central Minnesota and includes the Minnesota River and its tributaries. This region is underlain by Upper Cambrian and Lower Ordovician sedimentary rocks, including an indurated, ledge-forming Cambrian sandstone. A thick sequence of fine-grained, clast-poor, glacial diamicton overlies the bedrock (Lusardi et al. 2011). Diamictons are interbedded with glacial outwash and lacustrine sediments. The total thickness of the Quaternary sediment exceeds 150 m in some areas (Jirsa et al. 2011). The Minnesota River occupies the valley created by the drainage from glacial Lake Agassiz (Fig. 1) which incised up to 70 m through mostly glacial sediment. Tributaries are still responding to that local base-level change via knickpoint migration, headward erosion, and valley widening. Some knickpoints are bedrock waterfalls and sit within 5–10 km of the Minnesota River. On other tributaries,

Table 1 Landslides characteristics by region and across the entire study area

Metric	Southeast	Metro	Minnesota River	Red River	Lake Superior	All Regions
Region area (km^2)	13,000	5,200	22,400	29,300	16,600	86,500
Number of mapped landslides	738	537	3,365	2,648	2,446	9,734
Median area of each landslide (m^2) (IQR[1])	6,275 (14,241)	2,080 (3,757)	1,001 (2,412)	4,904 (11,427)	709 (1,570)	1,786 (4,792)
Median landslide slope - degrees (IQR[1])	35 (8)	29 (7)	37 (11)	14 (7)	30 (8)	33 (11)

[1] *IQR refers to the interquartile range calculated as the difference between the 75th and 25th quartile*

steep knickzones exist for tens of kilometers upstream from their confluence with the mainstem Minnesota River (e.g. Gran et al. 2009; 2013).

4. The **Red River Region** in northwestern Minnesota lies within the watershed of the north-flowing Red River of the North and the former bed of glacial Lake Agassiz. The lake level dropped rapidly by ~9 ka, and the north-flowing Red River of the North became established in the former lake plain, incising and exposing up to 15 m of clay-rich lacustrine and nearshore sediments along its banks and those of its larger tributaries (Brevik 1994). Only a subset of the Red River watershed was mapped in this study due to time constraints.
5. The **Lake Superior Region** is in northeastern Minnesota along the north shore of the modern Lake Superior where erosion-resistant igneous bedrock is overlain by glacial deposits of varying thickness. Near the end of the last glaciation, the western end of Lake Superior was covered by a large proglacial lake called glacial Lake Duluth (Fig. 1), which had a water level up to 200 m higher than Lake Superior today (Breckenridge 2013). Glacial Lake Duluth left behind locally thick deposits of silt and clay, particularly in the western end of the lake, and when lake level fell, base level dropped for all of the tributaries draining into Lake Superior. On-going differential isostatic rebound has led to modern lake level rise on the western end of Lake Superior, impacting coastal erosion today (Breckenridge 2013).

3 Methods

3.1 Landslide inventory

DeLong et al. (2021) contains a landslide inventory dataset covering several landslide-prone regions of Minnesota that were identified by lidar mapping, field observation, and research into documented historical landslides (Fig. 1). Most of the landslides were identified and mapped using derivatives of 1-meter-resolution digital elevation models (DEMs) made from airborne lidar surveys (MN DNR 2009; 2011; 2012b; 2012c; 2012d; 2012e; 2013b) following procedures modified from the Oregon Department of Geology and Mineral Industries (DOGAMI) protocol (Burns and Madin 2009). Lidar derivatives were calculated with standard GIS tools and include shaded relief, slope (degrees), planform and profile curvature, aspect, and red relief maps. Shaded-relief maps were made with artificial lighting from both 45 and 315 degrees azimuth. Aerial and satellite imagery were used (Maxar 2012), including repeat historical imagery available in Google Earth Pro (Google 2025). Historical landslides were identified through the search of libraries and the web, newspaper archives, government agency reports, and other documentation (as cited in DeLong et al. 2021). In each region, the landslide inventory is considered complete as of 2021 within the delineated boundaries of each region for landslides visible at the 1:4000 scale on lidar or remote imagery.

Field checking of landslides was performed to confirm their presence and make interpretations of landslide activity and characteristics, and to map smaller landslides not visible from remote-sensing data. Field checks were used to determine landslide classification, estimate scarp height, determine materials and units involved in the failure, and make other observations relevant to interpretations of landslide processes. Landslides not visible in lidar data nor observed directly in the field are not included in the inventory. These may include small landslides, very shallow landslides that do not leave a visible topographic form, and episodic landslides that occur in steep channels such as debris flows or other mass movements that also may not leave a topographic indicator. Furthermore, some steep slopes may be eroding via soil processes, rilling, sheetflow and other processes without clear evidence of landslides and as such are not mapped as landslides.

Landslides were mapped with as much detail as the 1-meter resolution lidar products allowed. Many mapped landslides were classified using Varnes (1978) classification by material (debris, earth, rock) and movement type (fall, flow, slide (rotational or translational), topple, lateral spread, or complex) per protocols in Burns and Madin (2009). Scarp areas and deposits were mapped as separate polygons, and internal scarps were mapped as lines. In some cases, landslide deposits coalesce downslope of multiple scarp areas and were therefore mapped as a single deposit. When possible, attributes were assigned to landslides including information regarding the age, geologic material, landslide classification, and metrics such as slide area and average slope angle of the landslide area.

Slope angles were either surveyed in the field or measured from lidar elevations using a 3×3 grid cell neighborhood calculation. Where practical, the slope angle of adjacent unfailed areas were measured as a proxy for pre-failure slope angle. In most cases, the level of uncertainty of interpretations made about each slide is also provided. All data and metadata are available in DeLong et al. (2021).

3.2 Susceptibility analysis

To create landslide susceptibility maps, we performed statistical analyses of the landslide inventory with environmental variables representing potential causative factors including slope, aspect, elevation, relief, depth to bedrock, soil erodibility, substrate, land cover, and distance to streams. Susceptibility modeling was conducted first in the Lake Superior Region (Richard 2020), one of the more heterogeneous regions in terms of the type and thickness of glacial deposits and topographic relief. The Lake Superior Region was used as a prototype, and the results were used to inform modeling across all five regions.

The four most common quantitative methods used for landslide susceptibility modeling are logistic regression, neural networks, index-based models, and data overlay (Budimir et al. 2015; Reichenbach et al. 2018), and there are promising emergent methods using machine learning (Liu et al. 2023). We chose to use multivariate logistic regression because it has been shown to be the most reliable in several comparative studies (Aleotti and Chowdhury 1999; Guzzetti et al. 1999, 2006; Lee and Sambath 2006; Mancini et al. 2010; Yilmaz 2010; Ozdemir and Altural 2013). In the Lake Superior Region, we applied a multivariate logistic regression analysis, using a binary dependent variable — presence or absence of landslides from the inventory — and independent environmental variables, both numerical (e.g. slope) and categorical (e.g. lithology) (Richard 2020). From these results, we selected four environmental variables that were shown to have statistical significance in terms of predicting the presence or absence of landslides and were available across all study areas: slope, depth to bedrock (Jirsa et al. 2011), distance to lakes and streams defined as second order and greater (MN DNR 2012a; MN DNR 2013a), and lithology of the surficial unit as represented in the statewide Quaternary geologic map of Minnesota (MGS 2019).

To assess landslide susceptibility across all regions, we generated point data from our landslide inventory representing presence and absence of landslides. To collect an equal amount of "stable" (landslide not present) and "unstable" (landslide present) points, we created irregular grids of varying point spacing across the regions. Unstable points were gridded within the boundary of mapped landslide scarp polygons. In the case of the Red River Region, unstable points were gridded within the boundary of both scarp and deposit polygons from our inventory because landslides in this region were mapped almost entirely as deposits rather than scarps. Areas outside of mapped landslide scarp polygons, but within each region's mapping extent, were gridded with stable points. Each point was assigned values of the environmental variables of slope, distance to stream, depth to bedrock, and surficial lithology.

R statistical software (R Core Team 2022) was used for multivariate logistic regression analysis following methods in Richard (2020). Stable and unstable landslide point data were divided into 80% training data and 20% test data following Bai et al. (2010) and Eeckhaut et al. (2006). The logistic model can be expressed as

$$P = \frac{1}{1 + e^{(-z)}} \tag{1}$$

where P is the conditional probability that a landslide is present (1) or absent (0), and z is the linear logistic model

$$z = b_0 + b_1x_1 + b_2x_2 + \ldots + b_nx_n \tag{2}$$

where b_0 is the model intercept and b_i (i = 1,2,3,…n) are coefficients for independent variables x_i (i = 1,2,3,…n) (Lee and Sambath 2006; Chen and Wang 2007; Nandi and Shakoor 2009; Bai et al. 2010; Trigilia et al. 2015).

We implemented multivariate logistic regression analysis using independent environmental variables in a binary generalized linear model (glm) function for each separate region. For a given region, its multivariate model was iterated 1000 times to optimize best-fitting parameterization as identified by the Akaike Information Criterion (AIC). AIC works by comparing all possible iterated models with variations of included independent predictor variables. The lowest AIC value identifies the best fitting model from iterations using the fewest number of independent predictor variables without overfitting or underfitting test data (Akaike 1974). Once the model with optimal parameters was selected, accuracy was analyzed by applying a confusion matrix to test data to evaluate how well predicted values compared to real test values. Model accuracy is represented using values in the confusion matrix as

$$Accuracy\,\% = \frac{(True\ Negative + True\ Positive)}{(Total\ of\ all\ matrix\ values)} * 100 \tag{3}$$

where True Negative and True Positive are test values correctly predicted as stable and unstable, respectively.

The selected best-fitting parametrization for the multivariate model in each region was used to create its susceptibility map. Maps were created by weighting the four independent environmental variable rasters with best-fit coefficients for that region and calculating the landslide susceptibility every square meter in the study area. We then classified the susceptibility values as low (<0.5), moderate (0.5–0.6), higher (0.6–0.8), or highest (0.8-1.0) susceptibility according to natural breaks in the dataset using Jenks natural break classification. The contrast between the low susceptibility class and the moderate, high, and very high is stark – most low areas have values well below the 0.5 cutoff.

The input and output data for the susceptibility analysis had 1-meter spatial resolution, which can lead to unrealistically high-resolution maps of susceptibility. To counter this, susceptibility maps were filtered for short steep slopes unlikely to be a hazard; susceptible areas with an elevation change of less than 10 m over a 60 m distance were removed from the susceptibility results. However, in the Red River region where landslides commonly occur on lower topographic slopes, only susceptible areas having less than 3 m of elevation over a 60 m distance were removed. Lastly, a 10-m wide buffer was added to the mapped susceptible areas to visually emphasize that future landslides may cause erosion and deposition that propagates outside the areas of mapped susceptibility. This has a similar effect as mapping susceptibility at a coarser resolution than 1 m, as is common in most studies.

4 Results

4.1 Landslide inventory

Landslides are abundant in Minnesota: we mapped 9,734 landslides across the five regions (Fig. 2) (DeLong et al. 2021). Field checking indicated that lidar mapping was effective at identifying landslides. In the Lake Superior Region, for example, field checking of 702 landslides mapped remotely found that 685 (97.6%) were confirmed as landslides (Richard 2020). Within each region, landslides are not evenly distributed spatially (Fig. 2), and landslide density is concentrated in specific areas. When landslide density is calculated over 5 km^2 areas, it ranges from 0 to just over 10%, with higher landslide densities along river corridors (Fig. 3). The highest landslide densities were found along the Minnesota River valley and in lower reaches of tributaries to the Minnesota River, along the Red River of the North and its major tributaries, near the western tip of Lake Superior, and in upstream reaches of river valleys in the Southeast Region.

The size of the area impacted by a given landslide varied widely, from the smallest (11 m^2, in the Lake Superior Region) to the largest (245,608 m^2, in the Red River Region) mapped landslides. Landslide area reported here is the sum of the mapped headscarp and deposit polygon areas. Many smaller landslides were omitted as they were not identifiable in remote datasets. Median landslide areas for each region are evenly distributed across the range from smallest (709 m^2, Lake Superior Region) to largest (6,275 m^2, Southeast Region) (Table 1).

Median landslide areas of all regions are significantly different from each other (P=<0.001), except in the Southeast and Red River regions, which have the highest medians and largest ranges and are not significantly different from each other (Fig. 4). All regions have very large skewness in the distribution of landslide areas, which is why median and IQR were used to describe the variance. Specifically, all regions have numerous outliers with very large areas. Median slope angles fell into two distinct categories: the Red River

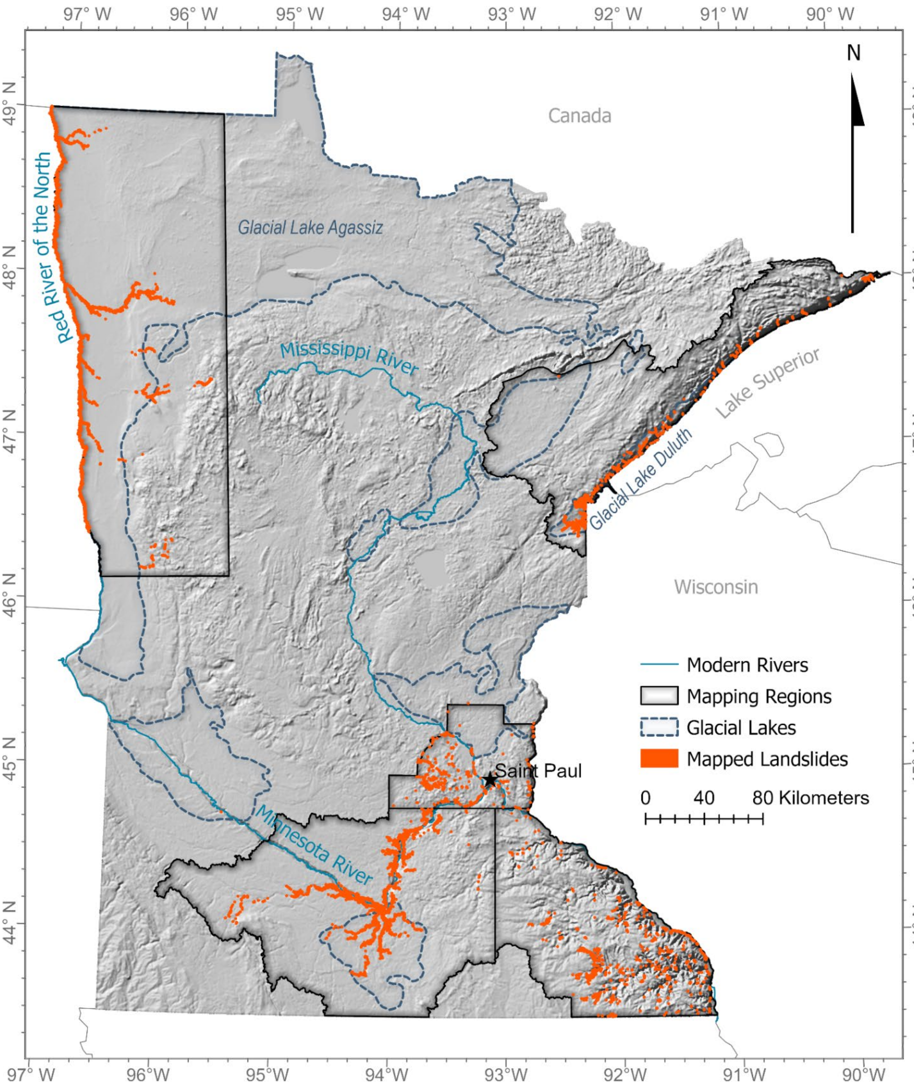

Fig. 2 Landslide inventory. Mapped landslides (DeLong et al. 2021) are enlarged for visibility. Base map is an exaggerated hillshade (z=30) (European Space Agency 2021)

region had a median landslide slope of 14° while the other 4 regional means were tightly clumped between 29° (Metro Region) and 37° (Minnesota River Region) (Table 1; Fig. 5).

4.2 Susceptibility modeling and mapping

The overall low relief and low slope of Minnesota is apparent by the susceptibility results. Four regions have only 1–2% of their areas calculated as moderate to high landslide susceptibility. The Southeast Region, which has older, more well-developed and high-relief fluvial valleys, has 8% of the study area with moderate to high landslide susceptibility (Online

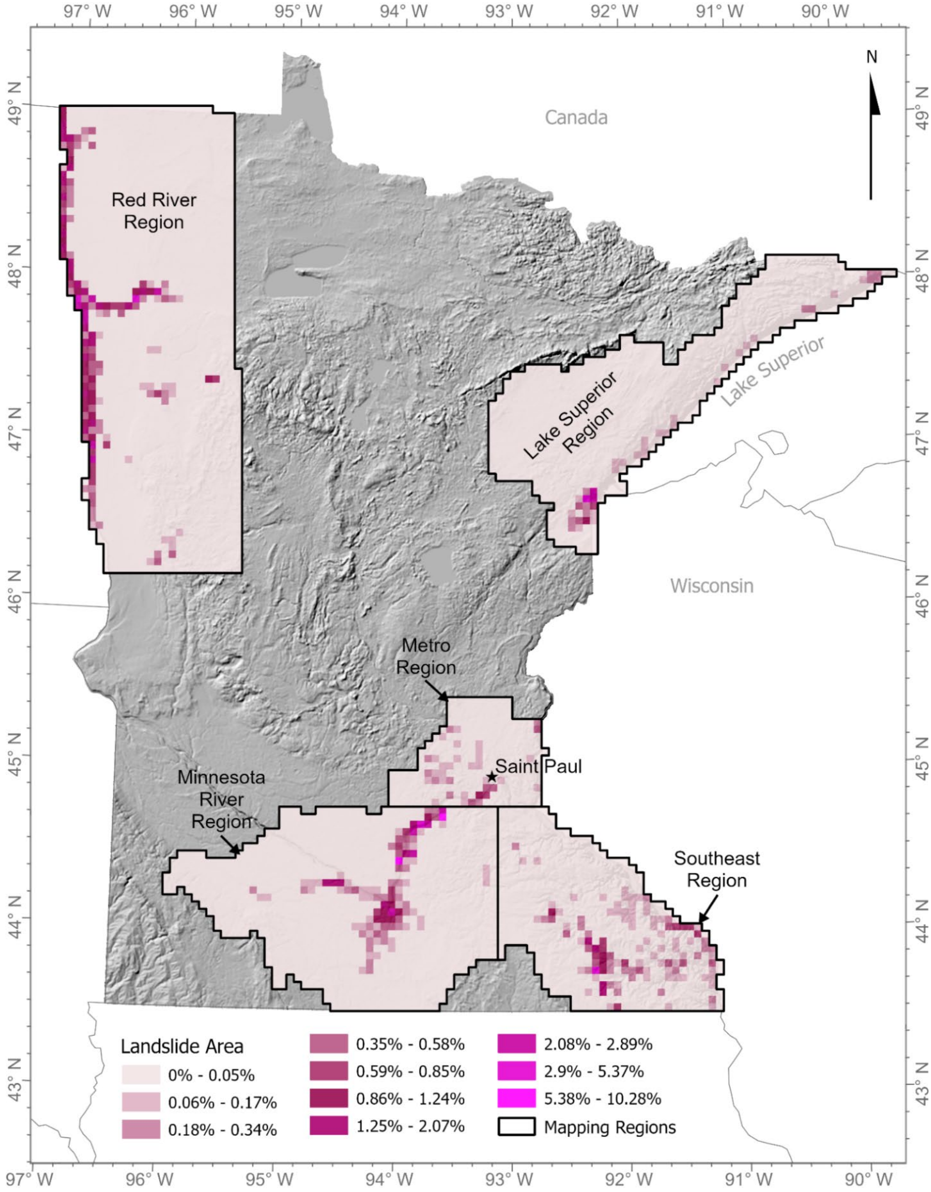

Fig. 3 Percent area mapped as landslides. Each 5 km^2 pixel portrays the % of surface area occupied by landslides in that grid cell. The landslide inventory was converted into a raster layer in-line with a 5-km grid, and the number of 1×1 m pixels in each 5-km grid was counted. In parts of the state that were not included in the landslide inventory, the base layer is an exaggerated hillshade (z = 30) (European Space Agency 2021)

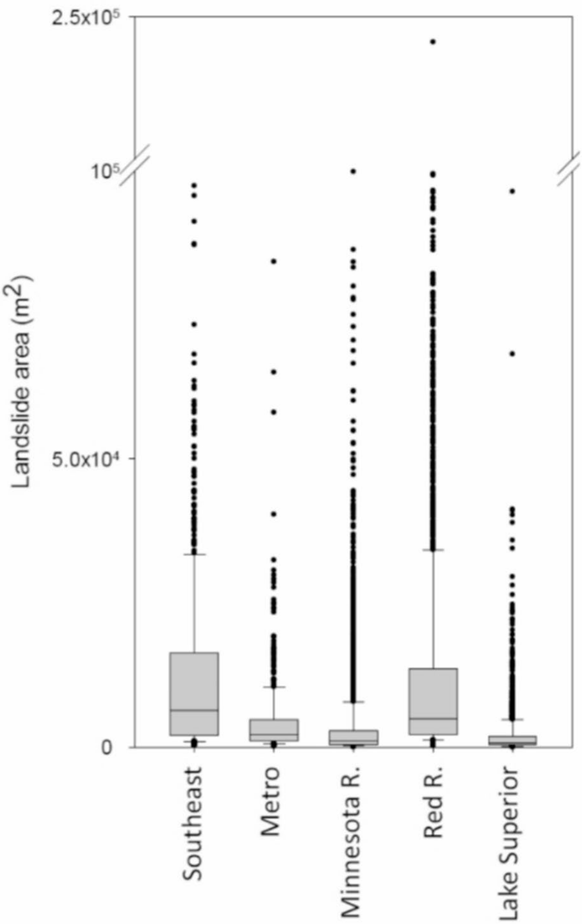

Fig. 4 Mapped landslide area by region. The box and whisker plot displays the median, the second and third quartiles (in the box), the 10th and 90th percentiles (the whiskers), and statistical outliers (points). Where a scarp and deposit were mapped separately, their areas were summed for the purpose of this analysis. In rare occasions, multiple scarps feed a single large deposit polygon; in those cases, the deposit and scarps were counted as a single landslide

Resource 1 Table S1). Logistic regression analyses identified the relative predictive power of several independent environmental variables in each region (Table 2). When the multivariate logistic regression coefficients are used to generate maps of landslide susceptibility (Hammer et al. 2025), a clear pattern emerges: the high susceptibility areas occur on steep slopes in river valleys, or adjacent to streams and lakes (Fig. 6). There are also isolated, often small areas of moderate to high landslide susceptibility where local slope is high farther from lakes or streams. These may be hummocky glacial moraine, ice-contact fans, eskers, bedrock outcrops, anthropogenic features, or other steep landforms. Landslide susceptibility data files are available in Hammer et al. (2025).

Steeper slopes consistently correspond with increased landslide susceptibility. Only small fractions of the regions' area had slopes greater than 10 degrees, ranging from 18% of the area in the Southeast Region to 2% in the Red River Region. Above a slope of 10 degrees, the logistic regression coefficient increases monotonically in all study regions (Table 2). This indicates that while the steepest slopes are the most susceptible to landslides, landslides may occur at lower slopes, as even slopes of 10–15 degrees have higher susceptibility than those below 10 degrees.

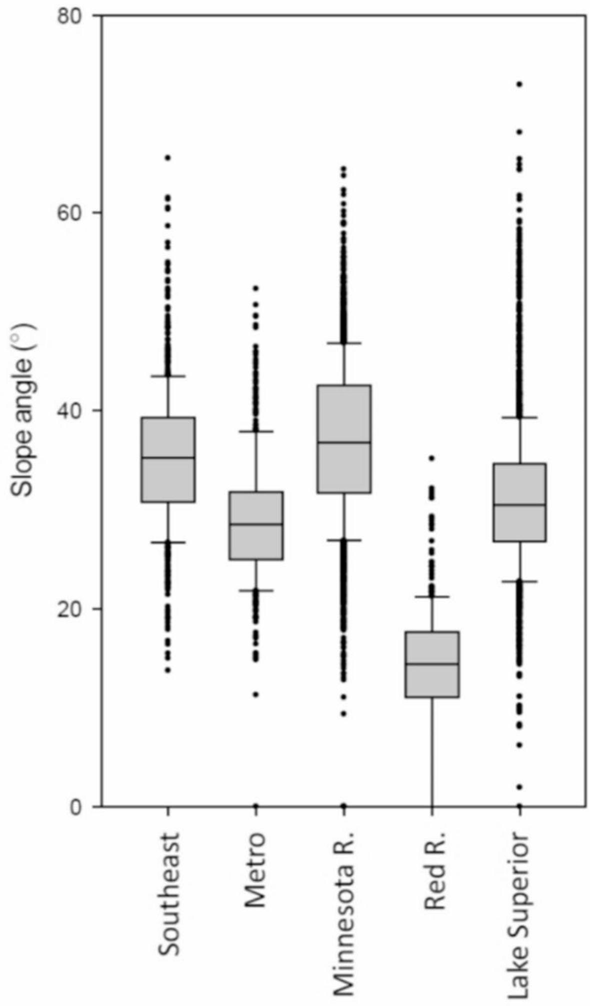

Fig. 5 Slope of mapped landslides, by region. The box and whisker plot displays the median, the second and third quartiles (in the box), the 10th and 90th percentiles (within the whiskers), and statistical outliers (points)

In all areas except the Southeast Region, distance to stream or lake also provided a relatively consistent indicator of landslide susceptibility in that landslide susceptibility decreases with distance away from stream or lake. In the Southeast Region, susceptibility gradually increases from 0 to 150 m from streams and lakes, reflecting the wider stream valleys, then begins to have an inverse relationship between distance and susceptibility beyond 150 m (see Fig. 7).

Depth to bedrock (or thickness of Quaternary sediment) does not have a consistent relationship with landslide susceptibility across all the regions. In the Southeast, Metro, and Lake Superior regions, thicker sediment corresponds with increased landslide susceptibility, but in the Minnesota River and Red River regions, landslide susceptibility decreases with increased depth to bedrock (Table 2). These are the two regions with the thickest surficial deposits, and the Red River Region had no bedrock exposed at all.

Table 2 Results from the susceptibility analysis, showing relative predictive power of independent variables in each region. Predictive power, or the regression coefficient, values indicate the positive or negative relationship between the dependent variable and independent variables. A greater, positive coefficient value indicates that variable, when all other variables are held constant, represents an environmental factor more likely associated with the presence of a landslide. The opposite is true of negative coefficient value

	Southeast				Metro				Minnesota River				Red River				Lake Superior			
Independent Variable	Coeff.	Std error	P value	Area (%)[2]	Coeff.	Std error	P value	Area (%)[2]	Coeff.	Std error	P value	Area (%)[2]	Coeff.	Std error	P value	Area (%)[2]	Coeff.	Std error	P value	Area (%)[2]
LR Intercept	-5.56	0.14	<0.01		-2.13	0.08	<0.01		1.01	0.08	<0.01		0.56	0.08	<0.01		-3.62	0.15	<0.01	
Lithology																				
Diamicton[1]	-	-	-	-	0	0	0	46.95	0	0	0	72.93	0	0	0	47.18	0	0	0	57.12
Sand	-	-	-	-	0.24	0.04	<0.01	48.29	0.59	0.04	<0.01	12.48	3.10	0.06	<0.01	28.75	0.21	0.14	0.14	19.58
Clay	-	-	-	-	-12.21	174.40	0.94	0.05	0.32	0.10	<0.01	3.10	1.06	0.07	<0.01	17.64	2.35	0.09	<0.01	11.54
Silt	-	-	-	-	-2.00	0.27	<0.01	2.13	0.08	0.06	0.17	11.22	2.95	0.08	<0.01	6.42	-0.22	0.21	0.28	6.57
Fill	-	-	-	-	-4.34	0.48	<0.01	1.31	-	-	-	-	-	-	-	-	-5.42	0.32	<0.01	2.16
Bedrock	-	-	-	-	-1.16	0.29	<0.01	0.16	-3.17	0.62	<0.01	0.19	-	-	-	-	-0.07	1.45	0.96	0.03
Gravel	-	-	-	-	-15.01	116.83	0.90	0.08	-15.35	82.62	0.85	0.08	-9.85	85.0	0.91	0.02	-4.96	0.70	<0.01	3.00
Loam	-	-	-	-	-	-	-	-	-	-	-	-	-	-	-	-	-	-	-	-
Boulders	-	-	-	-	-	-	-	-	-	-	-	-	-	-	-	-	-	-	-	-
Saprolith	-	-	-	-	-	-	-	-	-	-	-	-	-	-	-	-	-	-	-	-
Sediment	-	-	-	-	-0.27	0.24	0.25	1.03	-	-	-	-	-	-	-	-	-	-	-	-
Slope (Degrees)																				
Slope (0-10)[1]	0	0	0	82.41	0	0	0	92.60	0	0	0	96.94	0	0	0	97.7	0	0	0	91.7
Slope (10-15)	3.74	0.11	<0.01	7.02	3.20	0.05	<0.01	4.77	3.64	0.07	<0.01	1.47	3.55	0.08	<0.01	1.67	3.84	0.10	<0.01	4.80
Slope (15-20)	5.52	0.11	<0.01	3.96	5.22	0.06	<0.01	1.59	4.92	0.10	<0.01	0.68	4.44	0.12	<0.01	0.42	5.58	0.11	<0.01	1.88
Slope (20-25)	6.72	0.11	<0.01	2.85	6.74	0.08	<0.01	0.60	5.86	0.12	<0.01	0.42	5.73	0.20	<0.01	0.11	7.03	0.12	<0.01	0.81
Slope (25-30)	7.54	0.11	<0.01	2.20	7.84	0.11	<0.01	0.26	6.39	0.13	<0.01	0.26	6.41	0.32	<0.01	0.04	8.50	0.16	<0.01	0.38
Slope (30-90)	9.25	0.11	<0.01	1.56	9.49	0.16	<0.01	0.18	7.31	0.16	<0.01	0.23	7.24	0.44	<0.01	0.02	9.55	0.17	<0.01	0.38
Distance to Streams-Lakes (m)																				
Distance (0-25)[1]	0	0	0	5.38	0	0	0	15.09	0	0	0	6.19	0	0	0	7.74	0	0	0	7.13
Distance (25-50)	0.32	0.12	<0.01	3.23	-0.83	0.07	<0.01	4.75	-0.76	0.08	<0.01	2.59	-0.25	0.06	<0.01	2.86	0.15	0.16	0.35	2.77
Distance (50-100)	0.22	0.11	0.04	6.49	-1.95	0.07	<0.01	9.75	-1.52	0.08	<0.01	5.06	-1.21	0.05	<0.01	5.77	-0.79	0.15	<0.01	5.54
Distance (100-150)	0.44	0.11	<0.01	6.57	-2.70	0.08	<0.01	9.64	-2.07	0.09	<0.01	4.94	-2.53	0.06	<0.01	5.82	-1.35	0.16	<0.01	5.54
Distance (150-250)	0.19	0.10	0.05	13.10	-2.80	0.07	<0.01	17.25	-2.62	0.09	<0.01	9.53	-3.49	0.06	<0.01	11.55	-2.03	0.15	<0.01	10.9
Distance (250-500)	-0.90	0.10	<0.01	27.73	-2.86	0.07	<0.01	26.11	-3.35	0.08	<0.01	21.22	-5.50	0.08	<0.01	25.12	-2.11	0.14	<0.01	23.85
Distance (500-4,900)	-0.89	0.10	<0.01	37.49	-4.64	0.12	<0.01	17.41	-3.84	0.08	<0.01	50.46	-7.82	0.16	<0.01	41.14	-2.80	0.14	<0.01	44.29
Depth to Bedrock (m)																				
Depth (A-B)[1,3]	0	0	0	18.93	0	0	0	17.88	0	0	0	12.19	0	0	0	10.95	0	0	0	28.58
Depth (B-C)[4]	0.35	0.05	<0.01	31.32	0.24	0.08	<0.01	20.32	-0.28	0.06	<0.01	17.49	-0.04	0.06	0.52	11.37	0.14	0.09	0.14	26.92
Depth (C-D)[5]	0.50	0.05	<0.01	27.84	0.63	0.08	<0.01	20.35	-0.28	0.06	<0.01	15.56	-0.39	0.06	<0.01	12.88	0.30	0.10	<0.01	28.15
Depth (D-E)[6]	0.72	0.05	<0.01	21.90	1.11	0.08	<0.01	15.44	-0.22	0.06	<0.01	16.16	-1.04	0.06	<0.01	16.84	1.06	0.10	<0.01	16.35
Depth (E-F)[7]	-	-	-	-	1.94	0.08	<0.01	11.21	-0.19	0.06	<0.01	16.62	-2.17	0.06	<0.01	22.35	-	-	-	-
Depth (F-G)[8]	-	-	-	-	1.22	0.08	<0.01	14.79	-0.70	0.06	<0.01	21.98	-2.98	0.07	<0.01	25.61	-	-	-	-

[1] Coefficient of zero indicates this variable was used as a 'dummy variable', which other variables will be compared against

[2] Percent area of each independent variable in the susceptibility mapping region

[3] Depths A-B vary by each region's model, they are as follows: Southeast (0-2.04), Metro (0-29.0), Minnesota River (0-27.5), Red River (0-63.6), Lake Superior (0-1.22)

[4] Depths B-C vary by each region's model, they are as follows: Southeast (2.04-14.0), Metro (29.0-43.6), Minnesota River (27.5-41.5), Red River (63.6-75.5), Lake Superior (1.22-21.9)

[5] Depths C-D vary by each region's model, they are as follows: Southeast (14.0-31.7), Metro (43.6-59.4), Minnesota River (41.5-53.3), Red River (75.5-87), Lake Superior (21.9-45.5)

[6] Depths D-E vary by each region's model, they are as follows: Southeast (31.7-169), Metro (59.4-73.2), Minnesota River (53.3-65.5), Red River (87-100), Lake Superior (45.5-243)

[7] Depths E-F vary by each region's model, they are as follows: Southeast (NA), Metro (73.2-86.6), Minnesota River (65.5-82.3), Red River (100-118), Lake Superior (NA)

[8] Depths F-G vary by each region's model, they are as follows: Southeast (NA), Metro (86.6-190), Minnesota River (82.3-173), Red River (118-305), Lake Superior (NA)

A statewide, 1:500,000 scale map of surficial lithology from (MGS 2019) was used in the susceptibility analysis. It is important to note that the lithology referred to here is lithology mapped at the surface even though landslides may have occurred within deeper units. Some lithology categories, such as gravel, bedrock, and fill, are uncommon in this study area, and therefore tend to be statistically insignificant as indicated by high p-values (Table 2). The relationship between primary surficial lithology units that do have statistical significance and landslide susceptibility is not consistent between regions. In the Southeast Region, no statistically significant relationship was found between any lithology and landslide presence or absence, so we eliminated this variable from use in the final logistic regression equation there. In the Metro Region, 95% of the area is mapped as diamicton or sand, in roughly equal proportions, and they had similar landslide susceptibilities. In the Minnesota River Region, nearly 73% of the area is covered by diamicton, and most of the rest of the region is covered by sand or silt. Sand had a slightly higher susceptibility than silt or diamicton in this region. In the Red River Region, 47% of the area is diamicton, 29% is sand, 18% is clay, and 6% is silt. Sand and silt have higher susceptibility than clay, which in turn has slightly higher susceptibility than diamicton. In the Lake Superior Region, 57% of the area is covered by diamicton, 20% by sand, 12% by clay, and 7% by silt. Clay has the highest susceptibility of these lithologies.

Susceptibility maps were evaluated for accuracy by determining the number of original stable and unstable grid points that intersected areas mapped as susceptible. For all regions, the accuracy of comparing the multivariate susceptibility model results to the original sta-

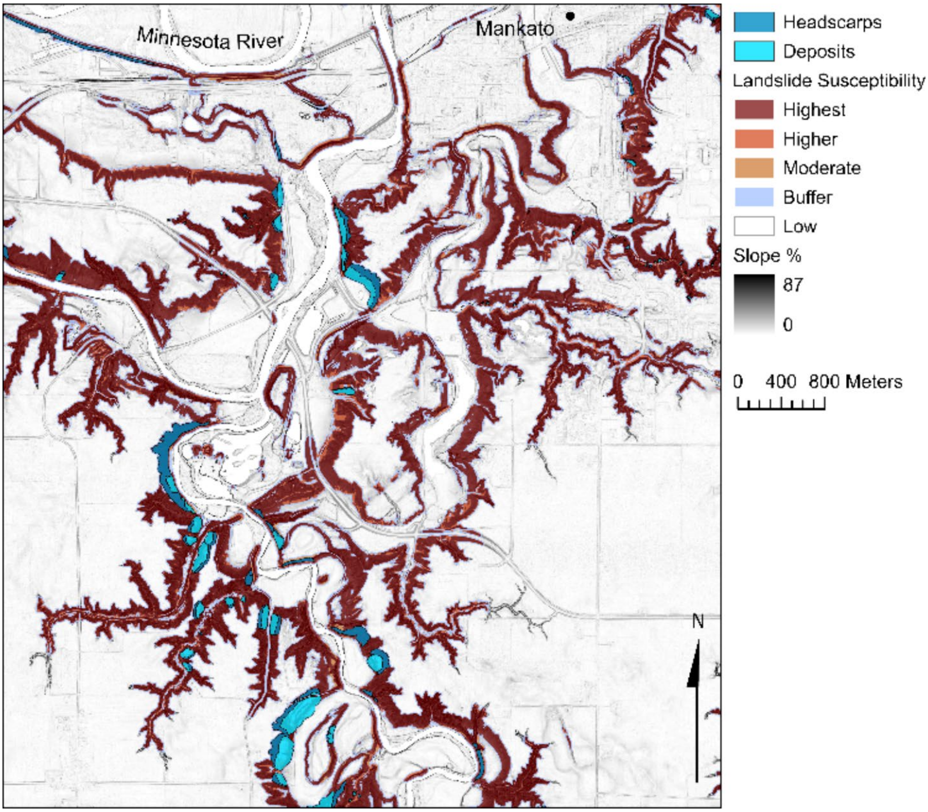

Fig. 6 Susceptibility map and inventory for portion of Minnesota River Region. See Fig. 1 for the location of the study regions

ble and unstable grid sampling points (Eq. 4) resulted in accuracies between 92 and 97% (Online Resource 1 Table S2).

4.3 Field observations and geologic context, by region

For each region of the study area, we describe our field observations and characteristics of the topography, bedrock stratigraphy, and surficial geology in the context of landslide occurrence (Figs. 2 and 3; Table 1) and results of the susceptibility analyses (Table 2; Hammer et al. 2025).

4.3.1 Southeast Region

The Southeast Region was not impacted by glaciers during the Wisconsinan glaciation, and it contrasts sharply with the other four regions in terms of landscape form: valleys are wider, relief is higher, and bedrock is closer to or at the surface (Fig. 7). Over 700 landslides were mapped in the Southeast Region, with most occurring on the steep bluffs along the Mississippi River and in upper reaches of the largest tributaries in the region, where landslides are

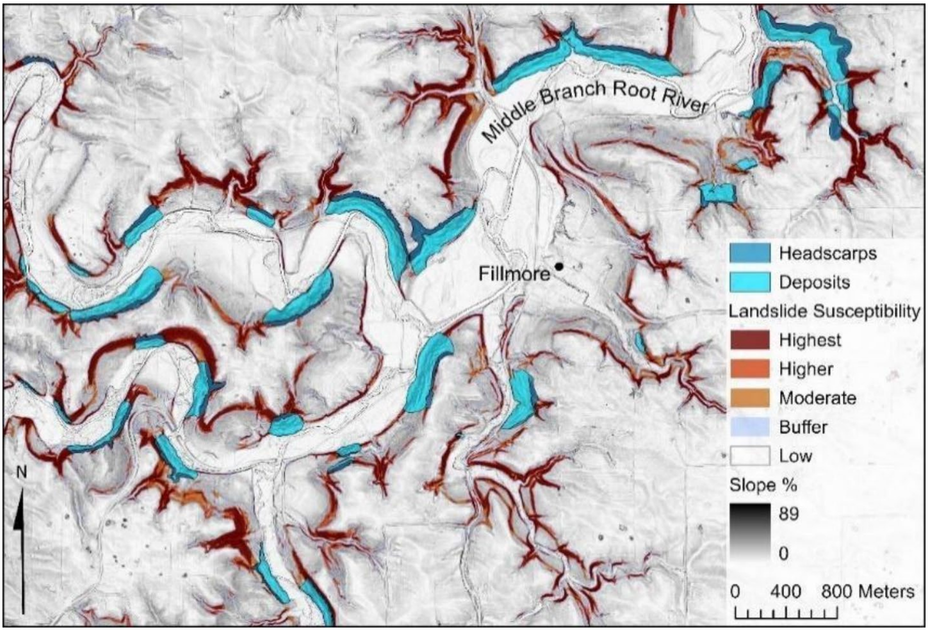

Fig. 7 Susceptibility map and landslide inventory for a portion of the Southeast Region. See Fig. 1 for the location of the study regions

formed in bedrock and colluvium (Figs. 2, 3 and 7). About 10% of mapped landslides in this region are rockfalls, the highest proportion in all five regions (DeLong et al. 2021). Rockfall deposits were seen along roadcuts, at the base of steep bedrock cliffs, and near seeps and springs. Small translational slides and earth and debris flows were seen primarily in tributary valleys. Those often involve upper layers of loess, thin glacial diamicton, or colluvium on slopes that move over weak sandstone or shale bedrock (Dean 2018). Rotational slides were also identified in places with loess overlying shallow bedrock.

The surficial geology of approximately 50% of the area is mapped as boulders and sediment: this is most commonly talus and colluvium on steep slopes. Most of the remainder of the area is mapped as diamicton and sand: generally, Illinoian or older glacial tills on uplands in the western part of the region and Quaternary alluvium on the valley floors (Jennings et al. 2007). None of these lithologic classes had statistical significance and were not used in the landslide susceptibility map of the region.

Higher depth to bedrock corresponds to higher landslide susceptibility in this region, as does higher slope. In this region, distance to streams and lakes is less systematically useful than in the other more recently glaciated areas: logistic regression coefficients increase until 150 m distance then decrease.

4.3.2 Metro Region

In the Metro Region, >500 landslides were mapped over an area of ~5,200 km^2. The most common types were shallow (generally less than 1–2 m depth) translational slides, large (10s of meters or more across) rotational slides with multiple failure planes, and rockfalls. In the Mississippi River gorge, we observed rockfall deposits that came from jointed carbonate units and near spring horizons although these were not easily distinguishable in the lidar data because of the near-vertical nature of the slopes. Along river bluffs in the region there are many small landslides. Away from major river valleys, shallow landslides are scattered on steep slopes in glacial sediment, including diamicton along lake shorelines and areas of focused overland flow.

Large rotational landslides are found along the bluffs flanking the Minnesota River valley (Fig. 8). Well logs and borings (Lusardi et al. 2016) show that multiple layers of glacial material were involved in these slides. The largest landslides have deposits that are either missing or obscured by more recent alluvial deposits.

Slope is the main control on landslide occurrence, with the highest positive coefficients in the multivariate model, even though over 92% of the area has slope less than 10 degrees, and 97% of the area has slope less than 15 degrees. The most susceptible areas occur along the bluffs of the Minnesota, Mississippi, and Saint Croix Rivers, and along the shores of lakes in glacial topography (Hammer et al. 2025).

4.3.3 Minnesota River Region

In the Minnesota River Region, 3,365 landslides were mapped over an area of ~22,000 km^2. Most are translational or rotational slides, though many are classified less specifically as "complex" slides interpreted to be partially composed of a translational or rotational component, a flow component, and multiple overlapping scarps and deposits suggesting reactivation over time. The zones of failure were predominantly clay-rich diamicton and sands. Headscarps are commonly vertical to sub-vertical in clay-rich glacial sediments. Rockfall deposits are present in layered Paleozoic sedimentary rocks where weaker rock layers underlie more competent layers or where groundwater emerges at a stratigraphic contact.

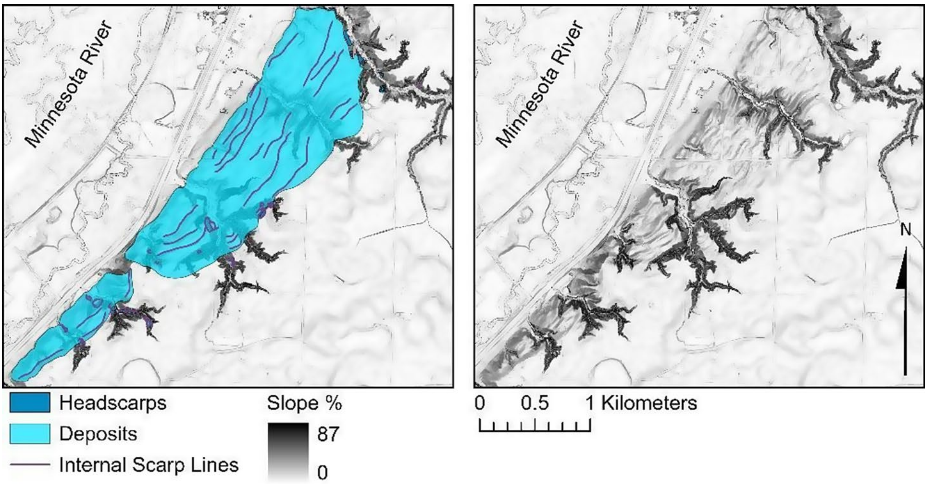

Fig. 8 Large rotational slides found along the valley walls in the Minnesota River valley in the Metro Region have younger ravines incising into them. The image on the left shows a slopeshade map with mapped slide locations. Deposits are missing and potentially buried by valley fill. The image on the right shows the texture of the slopeshade beneath the mapped slide locations. See Fig. 1 for the location of the study regions

Landslides in the Minnesota River valley occur on valley margins composed of diamicton or bedrock and on risers of stream terraces found throughout the valley (Fig. 6). The extensive tributary network in the Minnesota River Region has the highest landslide density (Figs. 3 and 6), with abundant landslides on terrace risers and valley walls in the incised lower reaches of tributary valleys.

Over 72% of the area in the Minnesota River Region is underlain by loam to clay-loam diamicton at the surface and much of the rest is underlain by sand or silt (MGS 2019). No significant differences exist between the apparent susceptibility of these lithologies. The strongest control on landslide occurrence is slope, with the highest positive coefficients in the susceptibility model, and the uplands in this area are particularly flat with nearly 97% of the area having slope < 10%. Most high susceptibility areas lie along river bluffs of the Minnesota River and its tributaries (Fig. 6). No apparent trend is observed in the relationship between landslide occurrence and depth to bedrock, which has a mean depth of 57 m.

4.3.4 Red River Region

In the Red River Region, 2,648 landslides were mapped over an area of > 29,000 km^2. Most are found on the outside of meander bends of the incised Red River of the North and its tributaries. The former lakebed is strikingly flat with nearly 98% of the region having slopes less than 10 degrees. The former lakebed has been incised by rivers and streams, and the laminated silt and illite- and smectite-rich glaciolacustrine clays (Johnson et al. 2016) exposed along these stream valleys are prone to slope failure. Away from the glacial lake plain, the region is underlain by diamicton, with increasingly hummocky topography eastward from the former lakebed. Landslides in the diamicton are similar to those found in the Minnesota River Region.

Landslides in the paleo-lakebed are associated with the < 10 m of relief created by stream incision. Slow drainage by clay-rich slopes can lead to high pore-water pressures during low flows, with many slopes moving during low summer and autumn river stages (Brooks 2003). Coherent slide blocks undergo a backward rotation and translation when underlying weak clays fail at the base of streambanks (Schwert 2003). The resulting landslide morphology mimics the “ridge and swale” morphology of depositional scroll bars within the valley bottom, and these can grade into one another, complicating lidar-based mapping efforts. Landslides occur on essentially every meander bend cutbank, often with multiple failure surfaces (Fig. 9). Because nearly all outside meander bends are landslides, some of these are among the largest landslide complexes mapped in this project. Many of the landslides are vegetated, which may indicate that they are stable or slow-moving over decadal timescales, but recent activity is a testament to the ability of landslide failures to propagate back beyond the vegetated streambanks (e.g. DeLong et al. 2022b).

The primary lithology for nearly half (47%) the area is diamicton, and the rest is sand (29%), silt (6%), and clay (18%) (MGS 2019). Sand, silt, and clay areas have slightly higher susceptibility than diamicton. Steeper slope is associated with increased landslide susceptibility. Shorter distance to lakes and streams is also associated with increased landslide susceptibility. Increased depth to bedrock, which ranges up to 305 m, is associated with decreased susceptibility, although bedrock is deeply buried throughout this region.

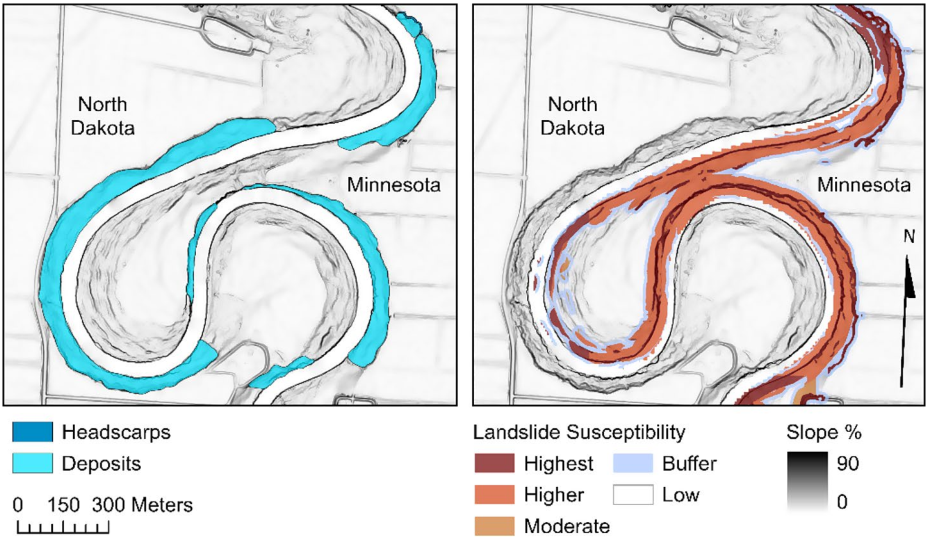

Fig. 9 Landslide inventory (left) and susceptibility map (right) for a portion of the Red River of the North, overlain over a slopeshade map. Note that the susceptibility mapping only occurred in the State of Minnesota on the east side of the river. In this image, headscarps are too narrow to be easily identified at this scale

4.3.5 Lake Superior Region

In the Lake Superior Region, 2,446 landslides were mapped over an area of > 29,000 km^2. Most of these occur along the lakeshore and within a few kilometers of Lake Superior along streams incised into bedrock and glacial sediment (Figs. 2 and 3). Landslides include rockfalls in exposed bedrock and translational and rotational landslides in glacial diamicton, glaciolacustrine, and nearshore sediments.

Depending on location, Lake Superior Region streams incise through glacial diamicton, glaciolacustrine (near-shore and deltaic sequences), and underlying bedrock. The complex paleo-shoreline and glaciolacustrine sediments deposited in an area occupied by glacial Lake Duluth (Fig. 1), now comprising the lower Saint Louis and Nemadji River watersheds, have heterogeneous and spatially discontinuous layers of clay, silt, and sand. These units are.

particularly prone to landslides, which is evident both in the landslide inventory (see Figs. 2 and 3) (DeLong et al. 2021), and in a study of landscape change resulting from a single severe summer storm in 2012 (DeLong et al. 2022a, b). In this area, landslides were so spatially dense that deposits often coalesced and aggraded the entire valley floor. Depth to failure plane was generally less than one meter, similar to the rooting zone of forests, and they manifest as steep translational slope failures and slumps that carried vegetation downslope.

Along the north shore of Lake Superior, landslides occur in the short, steep stream valleys leading to the lake and along the shoreline itself where glacial deposits and bedrock are subject to weathering and wave action. In this part of the region, nearly 20% of mapped landslides are rockfalls. These generally occur on steep exposures of jointed volcanic, hypabyssal, and plutonic rocks along stream valleys, road cuts, and along lake and inland cliffs. Talus from rockfalls are common at the base of larger cliffs in the region.

Most of the area is mapped as diamicton (57%), sand (29%), and clay (11%). The clay, much of which was deposited by former glacial lakes, is the most susceptible lithology in this region. As is the case in all regions, slope is a strong predictor of landslide activity. Areas within 50 m of streams and lakes are most susceptible to landslides, and susceptibility declines systematically with distance from streams and lakes. In the Lake Superior Region, depth to bedrock is skewed towards lower values, and areas with higher depth to bedrock, such as the glaciolacustrine and near-shore deposits southwest of Lake Superior, have higher susceptibility.

5 Discussion

Although Minnesota has relatively little topographic relief and lies in a tectonically stable location, it has a young, actively evolving landscape. Landslides are common, leading to loss of life and property damage. However, detailed landslide inventories and susceptibility models are rare in low-gradient landscapes like Minnesota's. The current national landslide inventory contains sparse data for low-gradient regions that experienced continental glaciation (Belair et al. 2022), and efforts to produce landslide susceptibility maps at national scales underestimate the extent of landslides in both Minnesota and North Dakota (Godt et al. 2012; Mirus et al. 2020, 2024). Those broad susceptibility mapping efforts often rely upon slope angle but also consider topographic relief, which can lead to the underprediction of landslide occurrence in low-relief areas with relatively short but steep slopes formed in weak unconsolidated materials. In addition, short, steep slopes may not be properly captured with more typically used 30-m gridded data (Woodard et al. 2023). Recent efforts to remedy this problem include a preliminary landslide susceptibility map for Canada, which indicates that some types of glacial sediments, especially glaciolacustrine and glaciomarine deposits, as well as shorter distance to coasts, lakes, and streams in low-relief, glaciated regions are important factors in increased landslide susceptibility (Dominguez-Cuesta and Bobrowsky 20132013). Also, a recent effort in North Dakota highlights extensive landsliding on steep slopes underlain by weak sediments and layered rocks (Shafer et al. 2024). The current study builds on those efforts and provides guidance for developing susceptibility maps in other post-glacial landscapes around the world.

The environmental variables used in our susceptibility model were chosen based on a detailed investigation in northeastern Minnesota, and then applied to the other four regions to generate susceptibility models fit to each region's data. We used the variability in those predictors to investigate differences in susceptibility drivers across the state. The predictor variables that arose as most important are, in part, directly related to the glacial history of the region in three ways that we list here and then describe in more detail below. First, the importance of distance to stream reflects that most of the landslides in the state are associated with high slopes in and around river valleys. In this post-glacial landscape, river incision is associated with changes in base level often driven by glacial lake drainage events. Second, in regions with wide variations in depth to bedrock, landslide susceptibility is higher in areas with greater depth to bedrock. Depth to bedrock is a measure of the thickness of surficial deposits, and in Minnesota, most of those deposits are glacially derived.

Lastly, landslides were often found to occur more commonly in specific lithologies, often diamicton or fine-grained fluvial, lacustrine or nearshore deposits, or observed in layered bedrock where weak layers underlie more resistant layers. Much of the surficial geology and shallow stratigraphy is related to glacial processes.

Slope is the most important factor in determining landslide susceptibility in all five study regions. The high slopes that drive landslides in Minnesota are often generated by glacial lake drainage and the ensuing incision by tributary streams flowing into those spillway valleys (e.g. Matsch et al. 1983; Gran et al. 2013; Faulkner et al. 2016; Hilgendorf et al. 2020). The drop in base level associated with these events rejuvenates the fluvial network, with incision still propagating upstream on rivers like the tributaries of the Minnesota River and rivers along the north shore of Lake Superior. Because of this, we also see a negative relationship between landslides and distance to streams in most regions. When deep incision occurs in a landscape underlain by erodible glacial sediments, knickpoint migration can be rapid. Knickpoints have migrated 40–60 km on some of the major tributaries of the Minnesota River since incision of the main valley by glacial Lake Agassiz overflow (Gran et al. 2009, 2013), and the high density of landslides in these tributary valleys shows up clearly in the landslide inventory (Fig. 3). The same relationship exists in the Lake Superior Region, where post-glacial lake level fall in Lake Superior caused inflowing rivers to deeply incise their channels. In the higher relief parts of the Lake Superior Region with thick glacial sediments, landslides are abundant. Elsewhere, rivers are incising into competent igneous bedrock, limiting the potential for landsliding. This may be why the environmental factor 'distance to streams' has a weaker relationship to landslide location in the Lake Superior Region compared with the Metro, Minnesota River, and Red River regions. The only region where distance to stream was inversely related to landslide susceptibility was the Southeast Region, where drainages have deeply incised but wide tributary stream valleys such that steep bluffs may sit farther from the active channel (Fig. 7).

Depth to bedrock is also an important factor influencing locations and types of landslides, and in most of the study region, thicker surficial deposits are associated with higher landslide susceptibility. Exceptions are observed in the Minnesota River Region, which shows little variability in susceptibility as a function of depth to bedrock, and in the Red River Region, where no bedrock is exposed. These regions both have thicker surficial deposits compared to the other regions, and glacial deposit thickness often exceeds the thickness of exposed sediment in bluffs.

Glacial stratigraphy has been shown to be important in landslide behavior (Perkins et al. 2017). Glacial deposits often include units with high cohesion and low hydraulic conductivity (like glacial till or glaciolacustrine deposits) interbedded with noncohesive sand and gravel with high hydraulic conductivities. Variability in cohesion impacts material behavior and variability of hydraulic conductivity impacts groundwater flow. Studies have found that even small contrasts in hydraulic conductivity can impact pore-pressure distribution and hillslope stability (Rulon et al. 1985; Reid and Iverson 1992). These effects can be exacerbated in river bluffs as floodwaters decline and focused shallow groundwater flow leads to failure of river bluffs (Simon et al. 2000; Fox and Wilson 2010; Perkins et al. 2017; Zhao et al. 2022). In addition, clay-rich sediments are particularly prone to failure as was observed in the Red River Region and elsewhere, with low-gradient slides often occurring in glaciolacustrine deposits (Giraud et al. 1991; Fletcher et al. 2002; Kohv et al. 2009; Badger and D'Ignacio 2018). The location and thickness of layers with varying cohesion and hydraulic conductivity can lead to deeper failures in places, especially where large hydraulic gradients exist and low conductivity layers outcrop near the base of slopes (Reid and Iverson 1992; Perkins et al. 2017).

One of the criteria for the choice of data used here to generate susceptibility models is that the dataset was available on a statewide basis. This limited our ability to incorporate stratigraphy into the susceptibility model. Field observations showed that glacial stratigraphy can be an important factor in any specific hillslope's susceptibility to landslides. The Minnesota River and Metro regions are predominantly underlain by interbedded glacial deposits, some of which have hydrologically restrictive layers that focus groundwater discharge. In some localities, these layers were observed to be destabilizing to hillslopes. In the western end of the Lake Superior Region, thick sequences of nearshore interbedded glaciolacustrine clays, silts, and fine sands have experienced abundant landslides. In fact, almost 75% of the mapped landslides in the Lake Superior Region were in the Saint Louis River and Nemadji River watersheds on the western end of the region (Richard 2020; DeLong et al. 2022a, b). Of those, at least 60% were in sediments mapped as glaciolacustrine. Conversely, in the northeast part of that region, landslides that formed in glacial till or clay often lack the interbedded sands seen in the nearshore glacial lake sediments, leading to a lower number of landslides per unit area (Fig. 3). Despite our observations that glacial stratigraphy is important, no statewide database exists at the appropriate scale to incorporate into our model, and therefore it could not be evaluated. Finer-scale "County Geologic Atlases" are available in some locations and can provide more detailed information regarding the local stratigraphy, local hydrologic conditions and other factors that would enhance landslide hazard analysis (MGS 2024). This serves as a reminder that these regional analyses cannot replace site-specific hazard assessments, and more focused field observations and measurements would aid in localized mitigation strategies.

Exposed bedrock can be an important driver for the occurrence and type of landslide. For example, landslides in the layered Paleozoic sedimentary rocks of the Southeast Region occur where weaker rocks underlie more resistant rocks, sometimes exacerbated by groundwater seepage causing weathering of the underlying rock. These rockfalls are difficult to map using lidar, but they are observable in the field in many parts of the state. Regions where bedrock outcrops at or near the surface, such as in the Southeast and Lake Superior regions, rockfalls made up a larger percentage of mapped failures (10.4% and 5.4%, respectively), although rockfalls were likely more common than represented in the inventory due to the difficultly mapping these deposits remotely.

Human activities can exacerbate landslide susceptibility. In the Metro Region, for example, slopes can be destabilized where stormwater runoff leads to concentrated flows and/or construction of buildings increases loading on slopes. In the Minnesota River and Red River regions, extensive land drainage has led to streams having higher peak discharges than they had prior to ~150 years ago (Schottler et al. 2014). Because landslides in these regions are predominantly along river corridors, floods and increased runoff can increase landslide frequency when fluvial erosion during floods undermines nearby slopes.

Heavy rainfall is often the trigger for landslides in Minnesota (e.g. DeLong et al. 2022a, b), and high-magnitude precipitation events were observed directly triggering landslides in multiple instances during the study (e.g. Kohout 2019). Climate models for the state and across the north-central United States project more and bigger storm events in the future (Harding and Snyder 2014; Liess et al. 2022; NCEI 2023; Wilson et al. 2023). Increased precipitation may lead to an increase in landslide activity due to excess surface runoff, saturation of near surface soils and sediment, and increased flood discharge (Gariano and Guzzetti 2016). Future work modeling the mechanics of failure in these regions could lead to prediction of triggering events, improving hazard mitigation efforts.

Because of the relatively coarse nature of the input environmental factor data used in the susceptibility modeling done in this study, susceptibility models do not quantitatively evaluate potentially important factors such as layered stratigraphy, local stormwater management, human modification of slopes, climate change, groundwater sapping, and stream channel processes. For specific locations, it is important to note that additional factors may be important to consider, and susceptibility maps cannot replace site-specific geotechnical investigations.

6 Conclusions

In the low-relief landscape of Minnesota, nearly 10,000 newly mapped landslides underscore the extensive nature of landslide hazards in formerly glaciated regions. Landslide susceptibility was primarily controlled by local slope, with distance to streams and depth to bedrock secondarily important. Field observations found that subsurface stratigraphy was important, though not quantifiable at the scale of this analysis. The presence of high slopes underlain by weak materials in Minnesota is directly attributable to glacial advances that deposited a wide range of sediments, glacial meltwater carved channels that lowered regional base level, and subsequent development of tributary stream networks incising into the glacial sediments. The ongoing development of tributary networks maintains and generates steep slopes where landslides occur today.

As climate and land-use change, these hazards may increase. This study offers a broad assessment of landslide hazards across Minnesota which provides new insight into landslide occurrence and susceptibility in a region that is not accurately modeled by national and international scale susceptibility modeling efforts (Godt et al. 2012; Stanley and Kirschbaum 2017; Mirus et al. 2020, 2024). This study uses data available across large regions, and site-specific assessments may be warranted to further assess risk in areas of elevated landslide susceptibility, especially to account for the complexities of layered glacial and bedrock stratigraphy. Future research could incorporate our findings with stratigraphy and cohesive strength of materials to create models for prediction and mitigation.

Supplementary Information The online version contains supplementary material available at https://doi.org/10.1007/s11069-025-07262-8.

Acknowledgements Thanks to A.D. Wickert, W.M. DeLong, M. Allison, A Dahlseid, D.T. Dahly, B.A. Dean, M. Endres, E. Fischer, K. Krippner, E. Kurak, S. Link, B Matti, R.W. Rehwinkel, A Senjem, B Sockness, J. VanBerkel, J.G. Willard and A.B. Williams for contributions to data collection and management. Funding for this project was provided by the Minnesota Environment and Natural Resources Trust Fund as recommended by the Legislative-Citizen Commission on Minnesota Resources (LCCMR). Additional funding was provided by: The U.S. Geological Survey Landslide Hazards Program, the Mary T. Dooley and James Goff endowments at the Minnesota State University, Mankato, and the Environmental Studies Program at Gustavus Adolphus College. Any use of trade, firm, or product names is for descriptive purposes only and does not imply endorsement by the U.S. Government.

Author contributions All authors contributed to the landslide mapping (field and/or remote). Susceptibility modeling was conducted by MH, SD, ZE, ER, and KG. Data analyses (including statistical analyses) were performed by LT, MH, and SD. LT, MH, SD, KG, and CJ wrote the manuscript, revised by all authors.

Funding for this project was provided by the Minnesota Environment and Natural Resources Trust Fund as recommended by the Legislative-Citizen Commission on Minnesota Resources (LCCMR). Additional funding was provided by: The U.S. Geological Survey Landslide Hazards Program, the Mary T. Dooley and James Goff endowments at the Minnesota State University, Mankato, and the Environmental Studies Program at Gustavus Adolphus College. Any use of trade, firm, or product names is for descriptive purposes only and does not imply endorsement by the U.S. Government. The authors have no relevant financial or non-financial interests to disclose. The authors have no competing interests to disclose.

References

Akaike H (1974) A new look at the statistical model identification. IEEE Trans Automatic Control 19(6):716–723. https://doi.org/10.1109/TAC.1974.1100705

Aleotti P, Chowdhury R (1999) Landslide hazard assessment: summary review and new perspectives. Bull Eng Geol Environ 58(1):21–44. https://doi.org/10.1007/s100640050066

Anderson FJ, Maike CA, Moxness LD, Murphy EC, Thapa N, York BC (2023) Areas of landslides in North Dakota. North Dakota Geological Survey. Retrieved from https://www.dmr.nd.gov/ndgs/landslides/

Associated Press (2023) Man dies in landslide at Minnesota State Park. https://apnews.com/article/minnesota-state-park-landslide-59d4c6a3e18c4bc7fe3d700aac4f15bd. Updated on December 3, 2023

Badger TC, D'Ignazio M (2018) First-time landslides in Vashon advance glaciolacustrine deposits, Puget lowland, USA. Eng Geol 243:294–307. https://doi.org/10.1016/j.enggeo.2018.07.011

Bai S, Wang J, Lu G, Zhou P, Hou S, Xu S (2010) GIS-based logistic regression for landslide susceptibility mapping of the Zhongxian segment in the three Gorges area, China. Geomorphology 115:23–31. https://doi.org/10.1016/j.geomorph.2009.09.025

Belair GM, Jones ES, Slaughter SL, Mirus BB (2022) Landslide inventories across the united States version 2: U.S. Geological survey data release. https://doi.org/10.5066/P9FZUX6N

Breckenridge A (2013) An analysis of the late glacial lake levels within the Western lake superior basin based on digital elevation models. Quat Res 80(3):383–395. https://doi.org/10.1016/j.yqres.2013.09.001

Brevik EC (1994) Isostatic rebound in the Lake Agassiz Basin since the late Wisconsinan. M.S. Thesis: University of North Dakota, 127 p

Brooks GR (2003) Alluvial deposits of a mud-dominated stream: the red river. Manit Can Sedimentology 50(3):441–458. https://doi.org/10.1046/j.1365-3091.2003.00559.x

Budimir MEA, Atkinson PM, Lewis HG (2015) A systematic review of landslide probability mapping using logistic regression. Landslides 12:419–436. https://doi.org/10.1007/s10346-014-0550-5

Burns WJ, Madin IP (2009) Special paper 42: Protocol for inventory mapping of landslide deposits from light detection and ranging (lidar) imagery. Oregon Department of Geology and Mineral Industries (DOGAMI). Retrieved from https://pubs.oregon.gov/dogami/sp/p-SP-42.htm

Chen Z, Wang J (2007) Landslide hazard mapping using logistic regression model in Mackenzie Valley, Canada. Nat Hazards 42:75–89. https://doi.org/10.1007/s11069-006-9061-6

Cloutier C, Locat J, Geertsema M, Jacob M, Schnorbus M (2016) Potential impacts of climate change on landslides occurrence in Canada. Slope safety preparedness for impact of climate change, 1st edn. CRS, pp 71–104

R Core Team (2022) R: A language and environment for statistical computing. R Foundation for Statistical Computing, Vienna, Austria. Ver. 2022.12.0.353. https://www.R-project.org/

Cossart E, Mercier D, Decaulne A, Feuillet T, Jónsson HP, Sæmundsson Þ (2013) Impacts of post-glacial rebound on landslide Spatial distribution at a regional scale in Northern Iceland (Skagafjörður). Earth Surf Processes 39(3):336–350. https://doi.org/10.1002/esp.3450

Day SS, Gran KB, Belmont P, Wawrzyniec T (2013) Measuring bluff erosion part 1: terrestrial laser scanning methods for change detection. Earth Surf Processes 38(10):1055–1067. https://doi.org/10.1002/esp.3353

Dean B (2018) Landslide hazard assessment of southeastern Minnesota. Thesis, Winona State University

DeLong SB, Engle ZT, Hammer MN, Jennings CE et al (2021) Inventory of landslides in the northwestern, northeastern, southern, and southeastern parts of Minnesota. U.S. Geological Survey. https://www.usgs.gov/data/inventory-landslides-northwestern-northeastern-southern-and-southeastern-parts-minnesota

DeLong SB, Hammer MN, Engle ZT, Richard EM, Breckenridge AJ, Gran KB, Jennings CE, Jalobeanu A (2022a) Regional-scale landscape response to an extreme precipitation event from repeat lidar and object-based image analysis. Earth Space Sci 9(12):1–34. https://doi.org/10.1029/2022EA002420

DeLong SB, Jennings CE, Gran KB (2022b) Landslides in Minnesota. US Geological Survey Fact Sheet 2022–3007. https://doi.org/10.3133/fs20223007

Domínguez-Cuesta MJ, Bobrowsky PT (2013) Proposed landslide susceptibility map of Canada based on GIS. Landslide Science and Practice: Volume 3: Spatial Analysis and Modelling, pp.375–382

Eeckhaut M, Vanwalleghem T, Posen J, Gover G, Verstraeten G, Vandekerckhove L (2006) Prediction of landslide susceptibility using rare events logistic regression: a case-study in the Flemish Ardennes (Belgium). Geomorphology 76(3–4):392–410. https://doi.org/10.1016/j.geomorph.2005.12.003

European Space Agency, Sinergise (2021) Copernicus Global Digital Elevation Model, distributed by OpenTopography. Retrieved from https://doi.org/10.5069/G9028PQB. Accessed 10 November 2023

Faulkner DJ, Larson PH, Jol HM, Running GL, Loope HM, Goble RJ (2016) Autogenic incision and terrace formation resulting from abrupt late-glacial base-level fall, lower Chippewa river, Wisconsin, USA. Geomorphology 266:75–95. https://doi.org/10.1016/j.geomorph.2016.04.016

Fletcher L, Hungr O, Evans SG (2002) Contrasting failure behaviour of two large landslides in clay and silt. Can Geotech J 39(1):46–62. https://doi.org/10.1139/t01-079

Fox GA, Wilson GV (2010) The role of subsurface flow in hillslope and stream bank erosion: A review. Soil Sci Soc Am J 74(3):717–733. https://doi.org/10.2136/sssaj2009.0319

Gariano SL, Guzzetti F (2016) Landslides in a changing climate. Earth Sci Rev. https://doi.org/10.1016/j.earscirev.2016.08.011

Geertsema M, Cruden DM, Clague JJ (2017) The landslide-modified glacimarine landscape of the Terrace–Kitimat area, BC. In: Slaymaker O (ed) Landscapes and landforms of Western Canada. World Geomorphological landscapes. Springer, Cham, pp 349–361. https://doi.org/10.1007/978-3-319-44595-3_25

Giraud A, Antoine P, Van Asch TW, Nieuwenhuis JD (1991) Geotechnical problems caused by glaciolacustrine clays in the French alps. Eng Geol 31(2):185–195. https://doi.org/10.1016/0013-7952(91)90005-6

Godt JW, Coe JA, Baum RL, Highland LM, Keaton JR, Roth RJ (2012) Prototype landslide hazard maps of the conterminous united States. In: Eberhardt E, Froese C, Turner AK, Leroueil S (eds) Landslides and engineered slopes: protecting society through improved Understanding. Taylor & Francis Group, London, pp 245–250

Google (2025) Google Earth Pro v7.3. Minnesota. Landsat, Copernicus, Airbus, Maxar Technologies, CNES, USDA/FPAC/GEO, U.S. Geological Survey, NASA. http://www.earth.google.com [March 01, 2025]

Gran KB, Belmont P, Day SS, Jennings C, Johnson A, Perg L, Wilcock PR (2009) Geomorphic evolution of the Le sueur river, Minnesota, USA, and implications for current sediment loading. In: management and restoration of fluvial systems with broad historical changes and human impacts. Geol Soc Am Special Paper 451:119–130. https://doi.org/10.1130/2009.2451(08)

Gran K, Finnegan N, Johnson A, Belmont P, Wittkop C, Rittenour T (2013) Landscape evolution, Valley excavation, and terrace development following abrupt postglacial base-level fall. Geol Soc Am Bull 125(11–12):1851–1864. https://doi.org/10.1130/B30772.1

Guzzetti F, Carrara A, Cardinali M, Reichenbach P (1999) Landslide hazard evaluation: a review of current techniques and their application in a multi-scale study. Cent Italy Geomorphology 31(1–4):181–216. https://doi.org/10.1016/S0169-555X(99)00078-1

Guzzetti F, Reichenbach P, Ardizzone F, Cardinali M, Galli M (2006) Estimating the quality of landslide susceptibility models. Geomorphology 81(1–2):166–184. https://doi.org/10.1016/j.geomorph.2006.04.007

Guzzetti F, Mondini AC, Cardinali M, Fiorucci F, Santangelo M, Chang K-T (2012) Landslide inventory maps: new tools for an old problem. Earth Sci Rev 112(1–2):42–66

Hammer MN, DeLong SB, Richard E, Engle Z et al (2025) Landslide susceptibility modeling results and maps covering the northwestern, northeastern, southern, and southeastern parts of Minnesota. U.S. Geological Survey. https://doi.org/10.5066/P14XOJSM

Harding KJ, Snyder PK (2014) Examining future changes in the character of central U.S. warm-season precipitation using dynamical downscaling. J Geophys Res-Atmos 119(13):13116–13136. https://doi.org/10.1002/2014JD022575

Hilgendorf Z, Wells G, Larson PH, Millett J, Kohout M (2020) From basins to rivers: Understanding the revitalization and significance of top-down drainage integration mechanisms in drainage basin evolution. Geomorphology 352:1–17. https://doi.org/10.1016/j.geomorph.2019.107020

Jennings CE, Johnson MD (2011) The Quaternary of Minnesota. In: Ehlers (ed) Developments in Quaternary Sciences, Elsevier 15:499–511. https://doi.org/10.1016/B978-0-444-53447-7.00038-6

Jennings CE, Aber JS, Balco G, Barendregt R, Bierman PR, Rovey IICW, Roy M, Mason JA (2007) Mid-Quaternary in North America. In: Elias SA ed., Encyclopedia of Quaternary Science 2:1044–1051

Jennings CE, Presnail M, Kurak E, Meier R, Schmidt C, Palazzolo J, Jiwani S, Waage E, Feinberg JM (2016) Historical landslide inventory for the twin cities metropolitan area. Published by the Minnesota Department of Natural Resources Division of Ecological and Water Resources

Jennings CE, Waage ED, Kurak E, Blenkush A (2020) Hennepin County Landslide Hazard Atlas. Hazard Atlas-Natural 01 (NZA-N01), published by Hennepin County Emergency Management

Jirsa MA, Boerboom TJ, Chandler VW, Mossler JH, Runkel AC, Setterholm DR (2011) S-21 Geologic Map of Minnesota Bedrock Geology. Minnesota Geological Survey. Retrieved from the University of Minnesota Digital Conservancy. https://hdl.handle.net/11299/101466

Johnson MD, Adams RS, Gowan AS, Harris KL, Hobbs HC, Jennings CE, Knaeble AR, Lusardi BA, Meyer GN (2016) RI-68 Quaternary lithostratigraphic units of Minnesota. Minnesota Geological Survey. Retrieved from the University of Minnesota Digital Conservancy. https://hdl.handle.net/11299/177675

Kirschbaum D, Stanley T (2018) Satellite-based assessment of rainfall-triggered landslide hazard for situational awareness. Earths Future 6(3):505–523

Kirschbaum DB, Adler R, Hong Y, Hill S, Lerner-Lam A (2010) A global landslide catalog for hazard applications: method, results, and limitations. Nat Hazards 52:561–575. https://doi.org/10.1007/s11069-009-9401-4

Kohout M (2019) Mass wasting investigation and assessment in the midwest:case study of the Minnesota River Valley, New Ulm to St. Peter, Minnesota, USA. Thesis, Minnesota State University Mankato. https://cornerstone.lib.mnsu.edu/etds/936/

Kohv M, Talviste P, Hang T, Kalm V, Rosentau A (2009) Slope stability and landslides in proglacial varved clays of Western Estonia. Geomorphology 106(3–4):315–323. https://doi.org/10.1016/j.geomorph.2008.11.013

Korup O, Clague JJ, Hermanns RL, Hewitt K, Strom AL, Weidinger JT (2007) Giant landslides, topography, and erosion. Earth Planet Sc Lett 261:578–589. https://doi.org/10.1016/j.epsl.2007.07.025

Krueger R, Zoet LK, Rawling JE (2020) Coastal bluff evolution in response to a rapid rise in surface water level. J Geophys Res-Earth 125(10):1–16. https://doi.org/10.1029/2019JF005428

Lee S, Sambath T (2006) Landslide susceptibility mapping in the damrei Romel area, Cambodia using the frequency ratio and logistic regression models. Environ Geol 50:847–855. https://doi.org/10.1007/s00254-006-0256-7

Liess S, Twine TE, Snyder PK, Hutchison WD, Konar-Steenberg G, Keeler BL, Brauman KA (2022) High-resolution climate projections over Minnesota for the 21st century. Earth Space Sci 9(3):1–16. https://doi.org/10.1029/2021EA001893

Liu S, Wang L, Zhang W, He Y, Pijush S (2023) A comprehensive review of machine learning-based methods in landslide susceptibility mapping. Geol J 58(6):2283–2301. https://doi.org/10.1002/gj.4666

Lusardi B, Jennings C, Harris K (2011) Provenance of des Moines lobe till records ice-stream catchment evolution during Laurentide deglaciation. Boreas 40(4):585–597. https://doi.org/10.1111/j.1502-3885.2011.00208.x

Lusardi BA, Gowan AS, Meyer GN, Thorleifson LH (2016) OFR16-01, Quaternary stratigraphy of Minnesota: statewide cross-sections. Minnesota Geological Survey. Retrieved from the University of Minnesota Digital Conservancy. https://hdl.handle.net/11299/175912

Lusardi B, Gowan AS, McDonald JM, Marshall KJ, Meyer GN, Wagner KG (2019) S-23, Geologic map of Minnesota - quaternary geology. Minnesota Geological Survey. Retrieved from the University of Minnesota Digital Conservancy. https://hdl.handle.net/11299/208552

Mancini F, Ceppi C, Ritrovato G (2010) GIS and statistical analysis for landslide susceptibility mapping in the Daunia area, Italy. Nat Hazards Earth Syst Sci 10:1851–1864. https://doi.org/10.5194/nhess-10-1851-2010

Mason JA, Nater EA, Hobbs HC (1994) Transport direction of Wisconsinan loess in southeastern Minnesota. Quat Res 41(1):44–51. https://doi.org/10.1006/qres.1994.1005

Matsch CL, Teller JT, Clayton L (1983) River Warren, the southern outlet to glacial Lake Agassiz. Glacial Lake Agassiz: Geological Association of Canada Special Paper 26:231–244

Maxar (2012) WorldView 2 imagery dataset. Retrieved from https://evwhs.digitalglobe.com/myDigitalGlobe/login
MGS (2019) D-01 Surficial geology of Minnesota database. Minnesota Geological Survey, retrieved 2020 from https://mngs-umn.opendata.arcgis.com/
Mickelson DM, Acomb L, Brouwer N, Edil T, Fricke C, Haas B, Hadley D, Hess C, Klauk R, Lasca N, Schnieder AF (1977) Shoreline erosion and bluff stability along Lake Michigan and Lake Superior shorelines of Wisconsin. Wisconsin Coastal Management Program Technical Report. Retrieved from https://repository.library.noaa.gov/view/noaa/17241
Minnesota Geological Survey (MGS) (2024) County Geologic Atlas (CGA) program website. https://cse.umn.edu/mgs/county-geologic-atlas
Minnesota Department of Natural Resources (MN DNR) (2009) Lidar elevation data for southeast Minnesota, 2008. Retrieved from https://resources.gisdata.mn.gov/pub/data/elevation/lidar/county/
Mirus BB, Jones ES, Baum RL, Godt JW, Slaughter S, Crawford MM, Lancaster J, Stanley T, Kirschbaum DB, Burns WJ, Schmitt RG (2020) Landslides across the USA: occurrence, susceptibility, and data limitations. Landslides 17:2271–2285
Mirus BB, Belair GM, Wood NJ, Jones JM, Martinez SM (2024) Parsimonious high-resolution landslide susceptibility modeling at continental scales. AGU Adv. https://doi.org/10.1029/2024AV001214
MN DNR (2013b) Lidar elevation, Central Lakes Region, Minnesota 2012. https://resources.gisdata.mn.gov/pub/data/elevation/lidar/county/
MN DNR (2013a) Stream routes with Strahler stream order. Minnesota DNR - Division of Fisheries, retrieved from https://gisdata.mn.gov/dataset/water-strahler-stream-order
MN DNR (2012e) Lidar elevation data, Blue Earth County, Minnesota, 2012. Retrieved from https://resources.gisdata.mn.gov/pub/data/elevation/lidar/county/
MN DNR (2012d) Lidar elevation data, Red River of the North Basin, 2008–2010. Retrieved from https://resources.gisdata.mn.gov/pub/data/elevation/lidar/county/
MN DNR (2012c) Lidar elevation data, Twin Cities Metro Region, Minnesota, 2011. Retrieved from https://resources.gisdata.mn.gov/pub/data/elevation/lidar/projects/metro/
MN DNR (2011) Lidar elevation data, Minnesota River Basin, southwest Minnesota, 2010. Retrieved from https://resources.gisdata.mn.gov/pub/data/elevation/lidar/county/
MN DNR Fisheries Unit (2012a) DNY hydrography dataset. Minnesota DNR, retrieved from https://gisdata.mn.gov/dataset/water-dnr-hydrography
Lidar elevation, Arrowhead Region, MN DNR, Minnesota NE (2012b) 2011. Retrieved from https://resources.gisdata.mn.gov/pub/gdrs/data/pub/us_mn_state_mngeo/elev_lidar_arrowhead2011/metadata/metadata.html
Mohseni O (2018) Storm-induced slope failure susceptibility mapping. Research Project Final report 2018-05 for the Minnesota Department of Transportation, 34 p + Appendices
Mossler JH (2008) RI-65 Paleozoic stratigraphic nomenclature for Minnesota. Minnesota Geological Survey. Retrieved from the University of Minnesota Digital Conservancy. https://hdl.handle.net/11299/58940
Nandi A, Shakoor A (2009) A GIS-based landslide susceptibility evaluation using the bivariate and multivariate statistical analyses. Eng Geol 110(1–2):11–20. https://doi.org/10.1016/j.enggeo.2009.10.001
National Centers for Environmental Information (NCEI) (2023) National trends for temperature, precipitation, and drought. National Centers for Environmental Information. Retrieved from https://www.ncdc.noaa.gov/temp-and-precip/us-trends/tavg/win
Ozdemir A, Altural T (2013) A comparative study of frequency ratio, weights of evidence and logistic regression methods for landslide susceptibility mapping: Sultan mountains, SW Turkey. J Asian Earth Sci 64:180–197. https://doi.org/10.1016/j.jseaes.2012.12.014
Pánek T (2015) Giant landslides in low-gradient landscapes: a global perspective. Eng Geol Soc Territory 2:905–908. https://doi.org/10.1007/978-3-319-09057-3_156
Pathak YP, Prakash I, Dholakia MB (2023) Conventional and modern approaches in landslide susceptibility mapping: A methodological review. Int J Appl Eng Technol 5:2633–4828
Perkins JP, Reid ME, Schmidt KM (2017) Control of landslide volume and hazard by glacial stratigraphic architecture. Northwest Wash State USA Geol 45(12):1139–1142. https://doi.org/10.1130/G39691.1
Reichenbach P, Rossi M, Malamud BD, Mihir M, Guzzetti F (2018) A review of statistically-based landslide susceptibility models. Earth Sci Rev 180:60–91. https://doi.org/10.1016/j.earscirev.2018.03.001
Reid ME, Iverson RM (1992) Gravity-driven groundwater flow and slope failure potential: 2. Effects of slope morphology, material properties, and hydraulic heterogeneity. Water Resour Res 28(3):939–950
Richard E (2020) Landslides in northeastern Minnesota: Inventory mapping and susceptibility assessment. Thesis, University of Minnesota Duluth. Retrieved from https://conservancy.umn.edu/handle/11299/219396
Rulon JJ, Rodway R, Freeze RA (1985) The development of multiple seepage faces on layered slopes. Water Resour Res 21(11):1625–1636

Runkel AC (1996) Bedrock geology of Houston County, Minnesota. Minnesota Geological Survey. Retrieved from the University of Minnesota Digital Conservancy. https://hdl.handle.net/11299/92932

Schottler SP, Ulrich J, Belmont P, Moore R, Lauer JW, Engstrom DR, Almendinger JE (2014) Twentieth century agricultural drainage creates more erosive rivers. Hydrol Proc 28(4):1951–1961. https://doi.org/10.1002/hyp.9738

Schwert DP (2003) A geologist's perspective on the Red River of the North: history, geography, and planning/management issues. Proceedings: 1st International Water Conference, Red River Basin Institute, Moorehead, MN. Retrieved from: https://www.ndsu.edu/fargo_geology/documents/geologists_perspective_2003.pdf

Shafer B, Ajmera B, Upadhaya KR, Daigh ALM (2024) Assessment of factors leading to the failure of slopes in North Dakota. https://doi.org/10.1007/s10346-024-02211-1. Landslides

Simon A, Curini A, Darby SE, Langendoen EJ (2000) Bank and near-bank processes in an incised channel. Geomorphology 35(3–4):193–217. https://doi.org/10.1016/S0169-555X(00)00036-2

Stanley T, Kirschbaum DB (2017) A heuristic approach to global landslide susceptibility mapping. Nat Hazards 87:145–164

STATEMENTS & DECLARATIONS

Swenson MJ, Wu CH, Edil TB, Mickelson DM (2006) Bluff recession rates and wave impact along the Wisconsin Coast of lake superior. J Great Lakes Res 32(3):512–530. https://doi.org/10.3394/0380-1330(2006)32[512:BRRAWI]2.0.CO;2

Trigilia A, Iadanza C, Esposito C, Scarascia-Mugnozza G (2015) Comparison of logistic regression and random forests techniques for shallow landslide susceptibility assessment in Giampilieri (NE Sicily, Italy). Geomorphology 249:119–136. https://doi.org/10.1016/j.geomorph.2015.06.001

U.S. Geological Survey (2023) Physiographic divisions of the conterminous U.S. [Data set]. U.S. Geological Survey. https://doi.org/10.5066/P9B1S3K8

Varnes DJ (1978) Slope movement types and processes. analysis and control, Landslides

Wartman J, Montgomery DR, Anderson SA, Keaton JR, Benoît J, dela Chapelle J, Gilbert R (2016) The 22 March 2014 Oso landslide. Wash USA Geomorphology 253:275–288. https://doi.org/10.1016/j.geomorph.2015.10.022

Wickert AD, Anderson RS, Mitrovica JX, Naylor S, Carson EC (2019) The Mississippi river records glacial-isostatic deformation of North America. Sci Adv 5(1):1–7. https://doi.org/10.1126/sciadv.aav2366

Wilson AB, Baker JM, Ainsworth EA, Andresen J, Austin JA, Dukes JS, Gibbons E, Hoppe BO, LeDee OE, Noel J, Roop HA, Smith SA, Todey DP, Wolf R, Wood JD (2023) Ch. 24. Midwest. In: Crimmins AR, Avery CW, Easterling DR, Kunkel KE, Stewart BC, Maycock TK (ed), Fifth National Climate Assessment, U.S. Global Change Research Program, Washington, DC, USA. https://doi.org/10.7930/NCA5.2023.CH24

Woodard JB, Mirus BB, Crawford MM, Or D, Leshchinsky BA, Allstadt KE, Wood NJ (2023) Mapping landslide susceptibility over large regions with limited data. JGR Earth Surf 128(5). https://doi.org/10.1029/2022JF006810

Yilmaz I (2010) Comparison of landslide susceptibility mapping methodologies for Koyulhisar, Turkey: conditional probability, logistic regression, artificial neural networks, and support vector machine. Env Earth Sci 61:821–836. https://doi.org/10.1007/s12665-009-0394-9

Zhao K, Coco G, Gong Z, Darby SE, Lanzoni S, Xu F, Zhang K, Townend I (2022) A review on bank retreat: mechanisms, observations, and modeling. Rev Geophys 60(2), p.e2021RG000761

Authors and Affiliations

Laura D. Triplett[1] · Morena N. Hammer[2] · Stephen B. DeLong[2] · Karen B. Gran[3] · Carrie E. Jennings[4] · Zachary T. Engle[5] · Julie K. Bartley[1] · Dylan J. Blumentritt[6] · Andy J. Breckenridge[7] · Stephanie Day[8] · Melissa A. Kohout[9] · Phil H. Larson[9] · Jeni A. McDermott[10] · Emilie M. Richard[3]

✉ Laura D. Triplett
triplett@gustavus.edu

[1] Department of Environment, Geography and Earth Sciences, Gustavus Adolphus College, 800 W College Ave, St. Peter, MN 56082, USA

[2] U.S. Geological Survey, Moffett Field, CA, USA

[3] Earth and Environmental Sciences Department, University of Minnesota Duluth, Heller Hall 229, 1114 Kirby Dr, Duluth, MN, USA

[4] Department of Earth and Environmental Science, University of Minnesota, John Tate Hall, 116 Church St SE, Minneapolis, MN 55455, USA

[5] U.S. Geological Survey, Denver, CO, USA

[6] Department of Geoscience, Winona State University, 130 Pasteur Hall, 175 W Mark St, Winona, MN 55987, USA

[7] Department of Natural Sciences, University of Wisconsin-Superior, Barstow Hall 103A, Belknap St., and Catlin Ave, Superior, WI 54880, USA

[8] Department of Geosciences, North Dakota State University, 1340 Bolley Dr, Fargo, ND 58105, USA

[9] EARTH Systems Laboratory, Earth Science Programs, Department of Anthropology and Geography, Minnesota State University Mankato, Morris Hall 206, 1651 Warren St, Mankato, MN 56001, USA

[10] Earth, Environment, & Society Department, University of St. Thomas, OWS 153, 2115 Summit Ave, St. Paul, MN 55105, USA